Small polar hits against S. aureus

Lim, Andrew S. T.; Vincent, Isabel M.; Barrett, Michael P.; Gilbert, Ian

Published in:
ACS Omega

DOI:
10.1021/acsomega.9b02507

Publication date:
2019

Document Version
Publisher's PDF, also known as Version of record

ACS OMEGA

Article

Cite This: ACS Omega 2019, 4, 19199−19215

http://pubs.acs.org/journal/acsodf

Small Polar Hits against *S. aureus*: Screening, Initial Hit Optimization, and Metabolomic Studies

Andrew S. T. Lim,[†] Isabel M. Vincent,[‡] Michael P. Barrett,[‡,§] and Ian H. Gilbert*[,†]

[†]Drug Discovery Unit, Wellcome Centre for Anti-Infectives Research, Division of Biological Chemistry and Drug Discovery, University of Dundee, Dundee DD1 5EH, U.K.

[‡]Glasgow Polyomics, University of Glasgow, Wolfson Wohl Cancer Research Centre, Garscube Campus, Bearsden G61 1QH, U.K.

[§]Wellcome Centre for Molecular Parasitology, Institute of Infection, Immunity and Inflammation, University of Glasgow, Glasgow G12 8TA, U.K.

Supporting Information

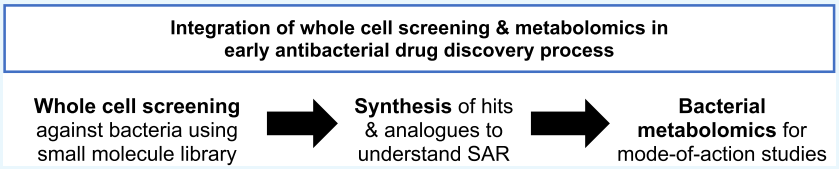

ABSTRACT: The global prevalence of antibacterial resistance requires new antibacterial drugs with novel chemical scaffolds and modes of action. It is also vital to design compounds with optimal physicochemical properties to permeate the bacterial cell envelope. We described an approach of combining and integrating whole cell screening and metabolomics into early antibacterial drug discovery using a library of small polar compounds. Whole cell screening of a diverse library of small polar compounds against *Staphylococcus aureus* gave compound **2**. Hit expansion was carried out to determine structure−activity relationships. A selection of compounds from this series, together with other screened active compounds, was subjected to an initial metabolomics study to provide a metabolic fingerprint of the mode of action. It was found that compound **2** and its analogues have a different mode of action from some of the known antibacterial compounds tested. This early study highlighted the potential of whole cell screening and metabolomics in early antibacterial drug discovery. Future works will require improving potency and performing orthogonal studies to confirm the modes of action.

INTRODUCTION

Antibacterial resistance, an issue under the umbrella term of antimicrobial resistance (AMR), is becoming a major global public health issue, affecting both developed and developing countries alike, although the impact in low and middle income countries is disproportionately high.[1−3] It has been estimated that the global death toll associated with AMR could rise to 10 million and the cumulative economic cost to U.S. $100 trillion by the year 2050 if AMR is not tackled urgently.[3]

Maintaining a healthy pipeline of new antibiotics is a key strategy in combating AMR as bacterial resistance against antibiotics is inevitable. An evaluation of the antibiotic pipeline by the Pew Charitable Trust[4] in September 2017 found that there were 48 antibiotics in various phases in clinical development. Despite these seemingly healthy numbers, there are several caveats to this observation. First, there is the risk of attrition in each phase of the clinical development of antibiotics.[5] Second, it was observed that most of the antibiotics in the pipeline were iterations of some of the major classes of antibiotics such as β-lactams, quinolones, tetracyclines, and oxazolidinones. This strategy, while maintaining a stream of new antibiotics, may suffer from the impact of cross-resistance, in which resistance against one antibiotic confers cross-resistance to other antibiotics of similar class, either through mutation of the molecular target or some common means of efflux or drug inactivation (e.g., β-lactamases).

As such, it is vital to maintain a healthy pipeline of antibiotics with either new modes of action or new chemical scaffolds. There have been a very few new classes of antibiotic uncovered since the golden age of antibiotic discovery (in the 1950s and 1960s),[6] and the introduction of new classes of antibiotics post-2000 (such as oxazolidinones, lipopeptides, and mutilins) can be traced to their discovery before 1990.[7]

A key issue in the development of new antibiotics is obtaining sufficient compound levels in cells, due to restricted permeation of the bacterial cell envelope and ejection of compounds through efflux pumps. The physicochemical properties of compounds play a role in compound uptake. The wealth of discussions[8−12] on the physicochemical properties of antibiotics and the comparison to other nonantibiotics highlights the challenges of designing an antibiotic with favorable physicochemical properties. The precise physicochemical properties required for cell entry are poorly understood. However, analysis suggests that antibacterial compounds tend to be more polar than other drugs,[10,12]

Received: August 6, 2019
Accepted: October 3, 2019
Published: November 4, 2019

with compounds acting against Gram-negative bacteria tending to be more polar/charged than those acting against Gram-positive bacteria. As such, the choice of libraries for screening bacteria is crucial to enhance the odds of finding hit compounds with the appropriate antibacterial physicochemical properties.

Current antibiotics target a limited set of enzymes or RNA structures within key bacterial cellular processes, such as cell wall biosynthesis, protein biosynthesis, and DNA biosynthesis. Although these targets are validated, there should be a search for other targets to treat bacteria resistant to current antibiotics.

There are two main routes to drug discovery, target-based and whole cell (phenotypic) approaches. Target-based discovery is hindered by the challenges of compound uptake/efflux, which means that compounds active in an enzyme assay are not necessarily active against intact bacteria. Further there is a risk that compounds that inhibit a single target can be subject to high rates of resistance. Whole cell approaches can also suffer from low hit rates due to compound uptake/efflux issues; however, compounds that are active hit essential targets and are able to accumulate to sufficient levels at those molecular targets. Whole cell hit discovery requires some degree of target deconvolution to ensure that whole cell actives are targeting a novel and/or progressible target. Knowledge of the binding mode of the lead in the protein is also valuable for compound optimization and to overcome issues such as poor pharmacokinetics.

Whole cell and target-based drug discovery processes are complementary and can be merged into a hybrid model (Figure 1). In this hybrid model, a library of compounds is

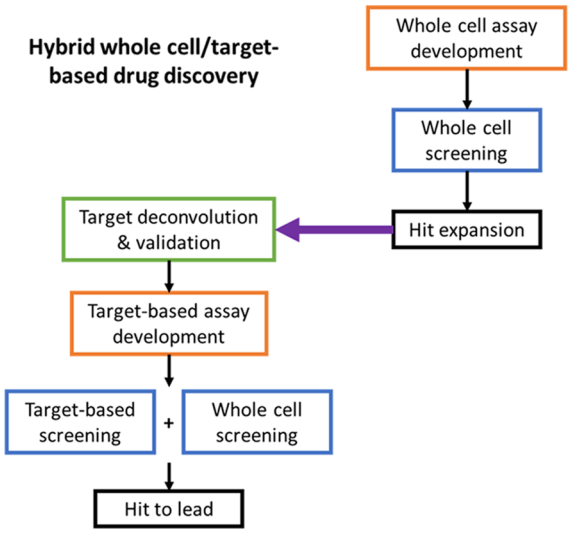

Figure 1. Steps involved in the hybrid whole cell/target-based drug discovery.

screened for whole cell activity. Hits from the screen are then expanded to give various analogues to probe for any indicative structure–activity relationship (SAR). Target deconvolution can then be used to identify the molecular target. If the target is suitable for development, target-based approaches can be used in optimization and scaffold hoping. This approach has the advantage of starting with compounds that are cell penetrant and which give rise to the desired whole cell response. The identified molecular targets possess a higher degree of validation, as it has been demonstrated that a druglike compound acting against this molecular target can have a desired whole cell effect on the bacteria.

We decided to screen against intact whole bacteria with a diverse library of small polar compounds,[10] which should address the physicochemical properties to some extent and being low molecular weight should cover a wide range of chemical space as well.[13,14] Furthermore, small polar fragment-like molecules would facilitate optimization toward lead-like molecules through the process of adding complexity.[15]

We decided to apply whole cell metabolomics as a way to compare modes of action, to be able to identify compounds that have a novel mechanism of action. Metabolomics can be described as a comprehensive bioanalytical technique to characterize and quantify metabolites of a biological system.[16] Metabolites reflect the biochemical status of the biological system. Since biochemical changes in a biological system lead directly to changes in its whole cell response, it follows that metabolomics can facilitate the understanding of the genotype–phenotype link, as changes in metabolite levels can be ascribed to changes in protein activity, which is linked to genes as well as to environmental status, where precursor metabolites are acquired by the cell. As such, the whole cell response upon exposure to an antibacterial compound is a function of the change in the metabolites. In some cases, this can be deconvoluted to reveal affected metabolic pathways and individual target enzymes. This should provide a fingerprint to allow comparison of the modes of action of different compounds and potentially, in some cases, ultimately the protein target. Some examples illustrate the use of metabolomics in this scenario.[17−21]

In this paper, we aim to describe the experience of using our in-house small, fragment-like polar compound library as the starting point in early antibacterial drug discovery. First, we aim to see if low-molecular-weight "fragment-like" compounds are a viable starting point for a drug discovery program and second can we use metabolomic fingerprints at this early stage of the discovery process to compare modes of action. We will present some early results, alongside thoughts and challenges that arose during the process.

RESULTS AND DISCUSSION

Whole Cell Screening of In-house Library. An in-house library of small, fragment-like polar molecules comprising of almost 1300 compounds has been described in detail by Ray et al.[22] The library consisted of a diverse set of small molecules, with physicochemical properties with low molecular weight [heavy atom count (HAC) 5−18]; low lipophilicity ($\log D \leq 2.5$ and $\log P \leq 2.5$), and aromatic rings ≤3 (these represent the upper limits; the median values are much lower). These physicochemical properties (low molecular weight and high polarity) should increase the chances of entry into the bacteria.[8] Further, the low molecular weight means that it is possible to cover a similar chemical space to libraries with much larger numbers of leadlike or druglike compounds. The library was curated to remove known structural alerts (toxicophores, reactives, and pan-assay interference compounds).[22] The library was mainly composed of commercially obtained fragments but also contained some proprietary compounds. The whole cell assay was based on measuring the turbidity of bacterial culture (as OD_{600nm}) as a proxy of growth. The screening was performed using 384-well plates to enable high-throughput screening. As an example of Gram-

DOI: 10.1021/acsomega.9b02507
ACS Omega 2019, 4, 19199−19215

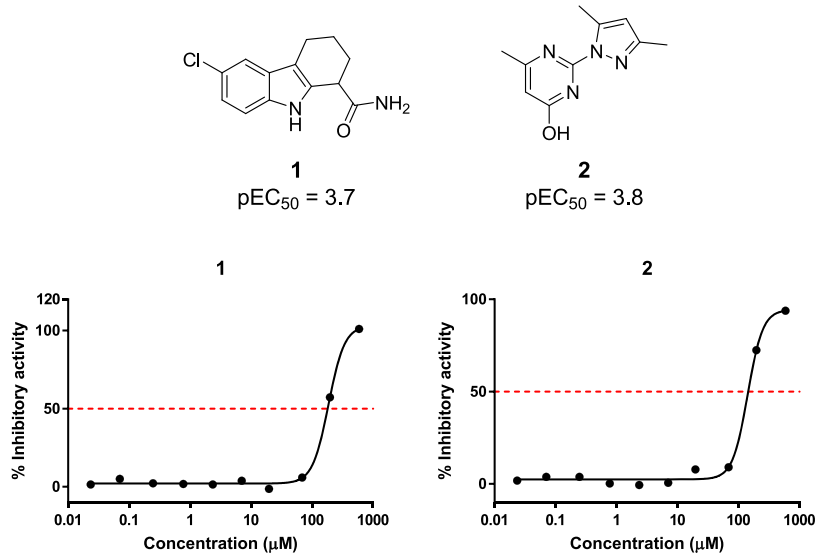

Figure 2. Dose–response curves of **1** and **2**, together with the corresponding structures and potency described as pEC_{50}.

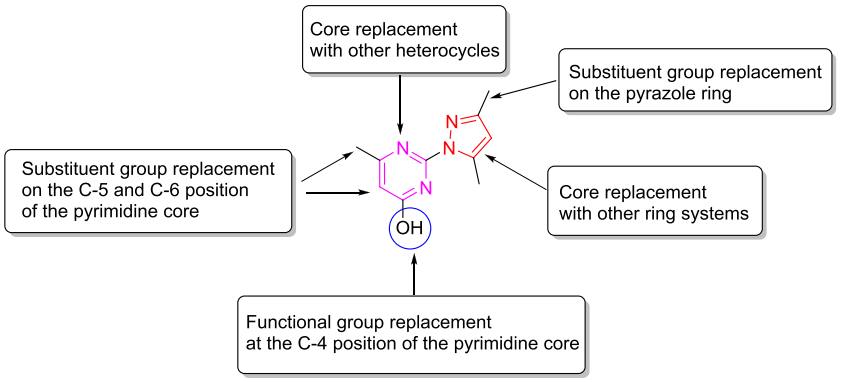

Figure 3. Possible strategies in generating analogues of **2**.

positive bacteria, *Staphylococcus aureus* RN4220, which was used in previous in-house screenings, was utilized in this whole cell assay. Compounds were initially screened at a single concentration of 600 μM to reflect the low molecular weight of these small fragment-like molecules.

From the single-point whole cell assay, 23 compounds were returned as hits, defined as having inhibitory activity at three robust standard deviations from the median. To remove false positives from the set of hits, a 10-point dose–response assay, with the top concentration of 600 μM, was performed at the whole cell level to seek any dose-dependent inhibitory activity and to estimate the potency of these hits. Of the 23 hits forwarded into the dose–response assay, two compounds, **1** and **2** (Figure 2), gave clear dose–response curves. Given their small size, they had a relatively low potency [pEC_{50} less than 4, where $pEC_{50} = -\log_{10}(EC_{50})$], which is not unexpected. However, the ligand efficiencies (LE – determined as 1.37 × pEC_{50}/heavy atom count) of the key hits were very promising, 0.30 and 0.35. By analogy with fragment-based drug discovery processes, the small size allows scope for optimization, while retaining ligand efficiency.

Compound **1** has been described in the literature as EX-527, a SIRT1 inhibitor.[23,24] Literature investigation revealed compound **2** to be a ligand of the adenosine A_{2A} receptor discovered using fragment-based drug discovery.[25,26] It was also described as a noncompetitive inhibitor of the human divalent metal transporter DMT1/SLC1 1A2, with the K_i of approximately 20 μM.[27] Interestingly, the pyrazolylpyrimidine scaffold of **2** was described as having fungicidal activity.[28,29] Additionally, **2** was described to be active against *Mycobacterium tuberculosis*.[30]

Hit expansion of **2** was carried out, as **2** has lower molecular weight and lipophilicity than **1** and a greater chemical tractability, thus allowing greater complexity to be added during the hit expansion process.

Resynthesis of 2 and Analogues. Compound **2** is a pyrazolylpyrimidine. The distribution of various tautomeric forms (pyrimidinone and hydroxypyrimidine) has been discussed[31] using various theoretical methods, albeit in the gaseous phase. A computational study on complexes of 4-hydroxypyrimidine with water suggested that the pyrimidinone (4-oxopyrimidine) tautomeric form predominates over the 4-hydroxypyrimidine tautomeric form at a 3:1 ratio at room temperature (rt).[32] Nevertheless, the hydroxypyrimidine representation will be used throughout this paper for consistency purposes and to aid visual comparison among the analogues synthesized.

A key early goal of the project was to validate the series and to try and increase its activity. The structure of **2** was amenable to derivatization, to probe the effect of various substituents at different locations on the scaffold, to increase potency (Figure 3). The choice of substituents for such a study was designed in

DOI: 10.1021/acsomega.9b02507
ACS Omega 2019, 4, 19199–19215

Scheme 1. Synthesis of 2 and Analogues from 2,4-Dichloropyrimidine Derivatives[a]

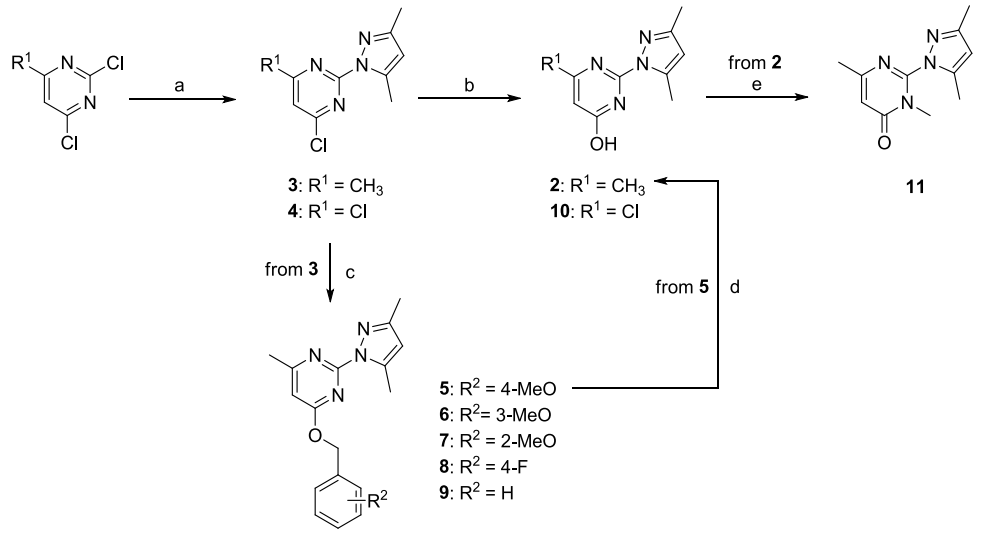

[a]Reagent and conditions: (a) 3,5-dimethylpyrazole, dioxane, microwave (MW) 150 °C, 3 h, 24−35%; (b) 1 M NaOH (aq), tetrahydrofuran (THF), MW 150 °C, 0.5 h, 68−90%; (c) appropriate benzyl alcohol, Cs_2CO_3, MeCN, reflux, overnight, 36−79%; (d) 1:1 trifluoroacetic acid (TFA)−dichloromethane (DCM), rt, 1 h, 72%; (e) MeI, K_2CO_3, dimethylformamide (DMF), reflux, overnight, 75%.

Scheme 2. Comparison of the Calculated Regio-isomeric Ratio of the Synthesis of 3 and 3b by Inclusion of the Base[a]

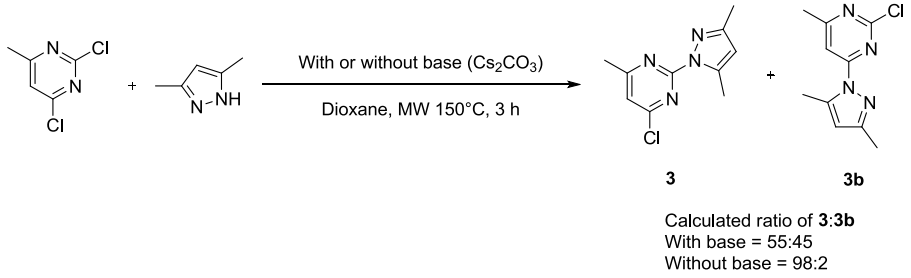

[a]Calculated ratio was based on NMR integration.

Scheme 3. Synthesis of Analogues of 2 from 2-Chloropyrimidine Derivatives[a]

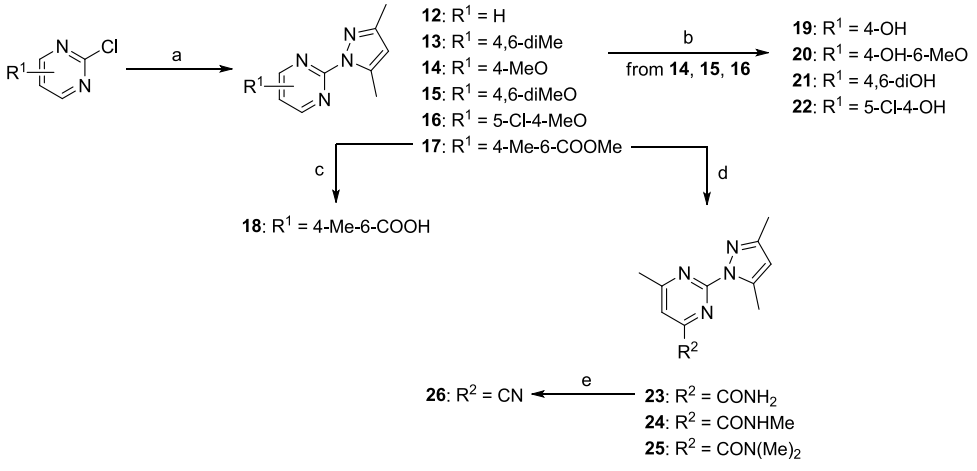

[a]Reagent and conditions: (a) 3,5-dimethylpyrazole, KOH, 18-crown-6, acetonitrile, room temperature, 1 day, 41−70%; or MW (80 °C, 15 min for **13**; 120 °C, 30 min for **14**), 32−47%; or for **17**: 3,5-dimethylpyrazole, Cs_2CO_3, dioxane, MW 150 °C, 3 h, 64%; (b) LiCl, DMF, MW 160 °C, 30 min (3 h for **21**), 24−97%; (c) LiOH−THF, rt, overnight, 87%; (d) NH_3 (for **23**) or $MeNH_2$ (for **24**) or Me_2NH (for **25**), MeOH, rt, overnight, 99−100%; (e) Burgess reagent, THF, rt, overnight, 93%.

a way that a simple change in the substituent can lead to changes in physicochemical properties such as lipophilicity, hydrogen bond donor and acceptor count, which will then impact compound activity. Various synthetic routes were generated to fulfill the various strategies highlighted in Figure 3.

DOI: 10.1021/acsomega.9b02507
ACS Omega 2019, 4, 19199−19215

First, the pyrazolylpyrimidine compounds were derived by reacting the pyrazole of interest with the appropriate pyrimidines. Substituted 2,4-dichloropyrimidines were used in the initial synthesis to generate the hit compound **2** and other analogues via the 4-chloro intermediate (for example, **3** and **4**) (Scheme 1).

The first step in Scheme 1 suffered from regio-isomerism, in which the displacement by the pyrazole derivative could occur at either the 2-position or the 4-position of the pyrimidine ring. Using the reaction to generate **3** as an example, it was interesting to note that the formation of the desired regio-isomer **3** was favored and enhanced without the presence of a base (Scheme 2). However, the isolated yield was compromised by the difficulty in separating both regio-isomers. The structure of these regio-isomers was distinguished by performing ^{1}H NMR experiments, in particular, nuclear Overhauser enhancement spectroscopy (Figures S1−S3).

Initially, it was envisaged that the synthesis of the hit compound **2** was carried out via the 4-methoxybenzyl ether derivative **5** through a TFA-mediated deprotection reaction. However, it transpired that direct hydroxylation of the 4-chloro derivatives (**3** and **4**) was also possible via microwave-assisted reaction with THF−NaOH solution, thus saving an additional step in generating analogues of **2**. Other benzyl ether derivatives **6**−**9** were generated, thus increasing the diversity of analogues. Additionally, the hit compound **2** was further methylated to give the *N*-methyl product **11**.

This synthetic scheme was extended to include 2-chloropyrimdine derivatives as precursors to other analogues with various substitutions on the 4- and 6-positions of the pyrimidine core (Scheme 3). For example, the methoxy derivatives **14**−**16** were demethylated to provide analogues **19**−**22**.

The methyl ester analogue **17** provided another attractive starting point for rapid hit expansion as it could be readily derivatized. Hydrolysis provided the free acid **18**, while displacement with simple amines provided various amides **23**−**25**. The primary amide was dehydrated to give the nitrile **26**. Note that these simple chemical transformations allowed us to generate various analogues with different physicochemical properties, in particular, hydrogen bond donor/acceptor count, which allowed a good assessment of SAR.

The pyrazole moiety was modified by replacing one of the methyl groups with a hydroxyl group. This was performed by using aminoguanidine as the precursor and reacting it with a β-keto ester[33] such as ethyl acetoacetate to give a pyrazolone derivative **28** (Scheme 4). The similar synthetic methodology gave the 4-methylpyrazolone derivative **29**. The β-keto ester precursor **27** was synthesized using a $TiCl_4$-mediated condensation reaction. The pyrazolone derivatives then underwent the ring formation reaction to create the desired pyrimidine core (**30** and **31**).

The pyrazole moiety was replaced entirely with cyclic saturated examples (Scheme 5). Three cyclic saturated structures were used as examples: pyrrolidine, 2-methylpyrrolidine, and morpholine. To achieve this, unsubstituted 1*H*-pyrazole-1-carboximidamide was used as a guanylating agent, attaching the guanyl group to the nitrogen atom of the cyclic saturated examples. These guanyl derivatives then underwent the usual ring formation reaction to give the analogues **35**−**37**.

This ring formation strategy was useful in exploring the effect of substitution on the 5-position of the pyrimidine core. The starting compound 3,5-dimethyl-1*H*-pyrazole-1-carboximidamide can be reacted with either β-keto ester **27** or acrylates to give analogues **38**, **39**, and **42** (Scheme 6). As with in Scheme 2, basic functional group transformation allowed the generation of analogues with diverse physicochemical properties. It was interesting to note that the ethyl ester **39** underwent transesterification to give **40** upon treatment of methanolic ammonia; thus, a different route was required to obtain the amide **41**. Direct synthesis of **42** gave a side reaction, which was documented in the literature,[34,35] thus an alternative route was envisaged in which the amide **41** was dehydrated to give **42**.

Scheme 4. Synthesis of 3 and Analogues from Pyrazolone Derivatives[a]

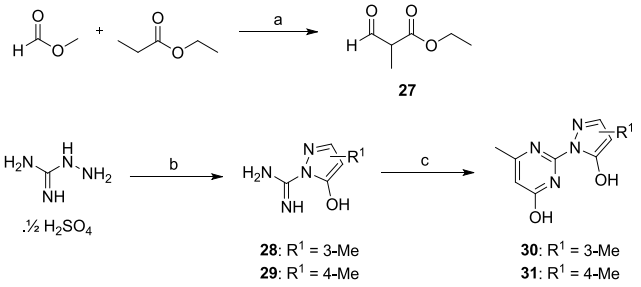

[a]Reagent and conditions: (a) $TiCl_4$, triethylamine (TEA), DCM, 0 °C to rt, 4 h, 63%; (b) ethyl acetoacetate (for **28**) or **27** (for **29**), NaOAc, H_2O, overnight (or 7 days for **29**), 52−64%; (c) ethyl acetoacetate, NaOEt, EtOH, reflux, overnight, 28−38%.

Attempts were also made to change the pyrimidine core for other heterocycles. At first, pyridine was used with 2,6-dichloropyridine derivatives as the starting point. The synthetic scheme (Scheme 7) is similar to Scheme 1, but the hydroxylation reaction required a copper-catalyzed reaction, modified from Yang et al.[36] and Wang et al.[37] There were limited number of pyridine examples, reasons of which will be discussed in the later sections.

All in all, these synthetic methodologies provided convenient methods to generate a diversity of analogues with varying pharmacophoric and physicochemical properties (examples shown in Figure S4). Furthermore, these synthetic methods can be applied in parallel synthesis, thus allowing rapid generation of analogues for SAR exploration.

Biological Evaluation of 2 and Its Analogues. The analogues synthesized (excluding intermediates **27**−**29** and **32**−**34**) were then tested using the 10-point dose−response whole cell assay against *S. aureus*. Here, we noted the challenges in evaluating biological activity for some of these analogues. First, due to the low potency nature of small fragment-like polar molecules, high concentrations were used during the whole cell screening process. The dose−response assay was performed with the modified top concentration of 1.8 mM, diluted threefold across 10 concentration points, to better visualize the curve. As we have a maximum in-house dimethyl sulfoxide (DMSO) concentration limit of 1% in whole cell screening assays, the stock concentration for such compounds was set to 200 mM. Unfortunately, analogues with substituents on the 5-position of the pyrimidines (for example **16**, **20**, **39**, **40**, and **42**) were found to be insoluble in DMSO at 200 mM.

The resynthesized **2** retained its inhibitory activity against *S. aureus* (Table 1). Some analogues have shown greater potency of almost a log fold than the original hit compound, in

DOI: 10.1021/acsomega.9b02507
ACS Omega 2019, 4, 19199−19215

Scheme 5. Synthesis Analogues of 2 by Replacing the Pyrazole with Saturated Ring System[a]

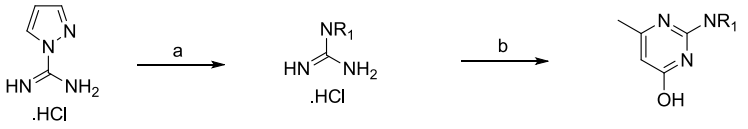

32: NR_1 = pyrrolidin-1-yl
33: NR_1 = 2-methylpyrrolidin-1-yl
34: NR_1 = morpholin-4-yl
35: NR_1 = pyrrolidin-1-yl
36: NR_1 = 2-methylpyrrolidin-1-yl
37: NR_1 = morpholin-4-yl

[a]Reagent and conditions: (a) various amines, TEA, MeCN, reflux, overnight, 74−85%; (b) ethyl acetoacetate, NaOEt, EtOH, reflux, overnight, 52−72%.

Scheme 6. Exploration of 5-Substituted Pyrimidine Analogues[a]

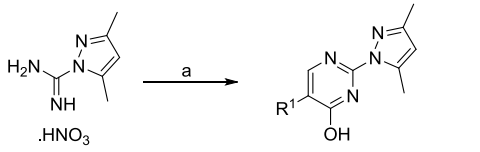

38: R^1 = CH_3
39: R^1 = COOEt
40: R^1 = COOMe
41: R^1 = $CONH_2$
42: R^1 = CN

[a]Reagent and conditions: (a) **27** (for **38**) or appropriate acrylates (**39** and **42**), NaOH, EtOH, 100 °C, overnight, 19−50%; (b) NH_3, MeOH, reflux, overnight, 102%; (c) NH_4OH, 75 °C, overnight, 86%; (d) Burgess reagent, THF, rt, overnight, 20%.

Scheme 7. Pyridine Analogues of 2[a]

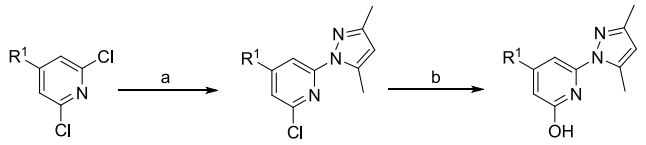

43: R^1 = CH_3
44: R^1 = H
45: R^1 = CH_3
46: R^1 = H

[a]Reagent and conditions: (a) 3,5-dimethylpyrazole, KOH, 18-crown-6, MeCN, MW 80 °C, 1.25−2.25 h, 50−55%; (b) tetrabutylammonium hydroxide, CuI, 8-hydroxyquinoline 1-oxide, H_2O, MW 180 °C, 3 h, 58−87%.

particular the benzyl ether analogues. Removal of the substituent groups on the pyrimidine core of the original hit **2** reduces the potency. The SAR on the pyrazole core is limited, with no other substituents having improved activity from the original 3,5-dimethyl substituents. The replacement of the pyrazole core with the saturated ring system removed any compound activity. The focused set of analogues that has been made cover a range of positions in the molecule and are sufficient to validate the hit and indicate potential ways to optimize the molecule. The overall SAR can be summarized in Figure 4.

As well as the potency of the compounds against *S. aureus*, various metrics were calculated. Ligand efficiency index (LEI)[38] is normally calculated for binding to a protein. LEI, defined as pEC_{50} divided by heavy atom count (HAC), is the simplification of LE in which the multiplier constant 1.37 was not applied in the equation. The value of LEI describes the extent of the improvement of the potency when more heavy atoms are added to the active compound. Originally used in the target-based fragment drug discovery, it can also be applied to whole cell screens where it measures how well each atom interacts with the molecular target and determines if substituents contribute significantly to the binding. Lipophilic ligand efficiency (LLE)[38] indicates whether the interactions are driven by lipophilicity (Table 2).

Although compound **5** was the most potent compound, much of the binding compared to compound **2** was probably driven by lipophilicity of the benzyl group, as shown by the drop in LLE. Compound **10**, on the other hand, had improved LEI and LLE compared to compound **2** and is the most efficient binder. It must be noted that compound **10** contains

Table 1. Activity of 2 and Its Analogues against *S. aureus*

compound	mean pEC_{50} (±SD)[a]	compound	mean pEC_{50} (±SD)	compound	mean pEC_{50} (±SD)
2	3.9 (±0.05)	**15**	NA	**31**	NA
3	3.8 (±0.07)	**16**	NS[c]	**35**	NA
4	3.2 (±0.05)	**17**	NA	**36**	NA
5	4.8 (±0.16)	**18**	NA	**37**	NA
6	4.7 (±0.01)	**19**	3.2 (±0.20)	**38**	2.8 (±0.03)
7	3.0 (±0.23)	**20**	NS	**39**	NS
8	3.6 (±0.70)	**21**	NS	**40**	NS
9	4.6 (±0.07)	**22**	NS	**41**	NA
10	4.4 (±0.04)	**23**	NS	**42**	NS
11	NA[b]	**24**	NA	**43**	NA
12	NA	**25**	NA	**44**	NA
13	3.0 (±0.17)	**26**	NA	**45**	NA
14	NA	**30**	NA	**46**	NA

[a]Expressed as the mean and its respective standard deviation from three replicates. [b]NA = no activity at 1.8 mM. [c]NS = not soluble in DMSO stock solution at 200 mM, hence not tested for compound activity.

DOI: 10.1021/acsomega.9b02507
ACS Omega 2019, 4, 19199−19215

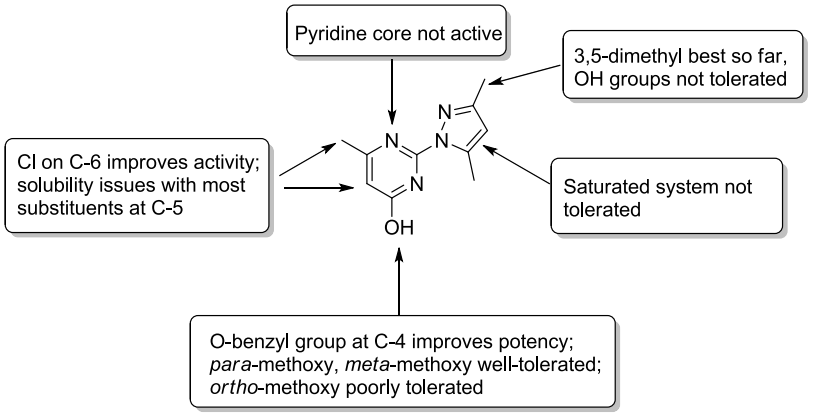

Figure 4. Summary of the SAR of **2**.

Table 2. Ligand Efficiency Analysis of Active Compounds

compound	MW	HAC[a]	clog *P*	mean pEC_{50}	LEI[b]	LLE[c]
1[d]	249	17	3.0	3.6	0.21	0.6
2	204	15	1.0	3.9	0.26	2.9
3	223	15	1.6	3.8	0.24	2.2
4	243	15	2.1	3.2	0.21	1.1
5	324	24	3.1	4.8	0.20	1.7
6	324	24	3.1	4.7	0.20	1.6
7	324	24	3.4	3.0	0.13	−0.4
8	312	23	3.2	3.6	0.16	0.4
9	294	22	2.8	4.6	0.21	1.8
10	225	15	1.2	4.4	0.30	3.2
13	202	15	1.5	3.0	0.20	1.5
19	190	14	0.6	3.2	0.24	2.6
38	218	16	0.5	2.8	0.18	2.3

[a]Heavy atom count. [b]Ligand efficiency index, defined as pEC_{50}/HAC. [c]Lipophilic ligand efficiency, defined as pEC_{50} − clog *P*. [d]Compound **1** was repurchased and retested for activity.

an α-chloropyrimidine, which is potentially chemically reactive. In addition, compound **10** is less lipophilic than compound **5**.

Metabolomics Study of 2 and Its Analogues and Other Relevant Compounds. The original hit **2** and the two selected compounds, **5** (highest potency) and **10** (highest LEI), were then subjected to metabolomics to elucidate any potential mode of action. Additionally, the other hit compound from the whole cell screening assay, **1**, was included in this metabolomics study. Two approved antibiotics, ciprofloxacin and trimethoprim, were also included in this study for comparison.

The metabolomics study was based on the kill-kinetic studies similar to those used by Vincent et al.,[17] in which the organism was exposed to an antibacterial agent and the effect monitored over time. The nature of the kill kinetics can be affected by the size of the starting inoculum and the dose of the compound administered at the beginning of the study.

S. aureus RN6390, which has been studied for its virulence and pathogenicity, was used, and it showed similar whole cell response and sensitivity to the RN4220 strain (examples in Table S1). Despite the subtle differences between the two strains RN6390 and RN4220, both were classified as methicillin sensitive and the lineage of these strains was traced back to NCTC8325 (also known as RN1) strain. This gave a hint of the whole cell similarity between the two strains and the capability of these compounds to target metabolic pathways. which are common and fundamental to these strains. The strain RN6390 has also been described to be virulent in various infection models[39−41] and capable of producing α-toxins. On the other hand, the strain RN4220, although is useful in genetic manipulation studies, may contain mutations, which may affect virulence factors and strain fitness,[42] and hence the change to the RN6390 strain for the metabolomics study.

The design of the metabolomics study was based on that of Vincent et al.[17] The minimal inhibitory concentration (MIC) of each compound in this metabolomics study was determined by the microdilution method (Table 3).

Table 3. Comparison of MIC Values among Various Compounds Showing Inhibitory Activity against *S. aureus* RN6390

compound	MIC (μg/mL)[a]
1	64
2	32
5	4
10	16
ciprofloxacin	0.25
trimethoprim	2

[a]Determined through the microdilution method in Luria−Bertani (LB) media.

Using 4 times the MIC as the starting dose, the bacteria were inoculated and incubated in fresh LB media for 2 h prior to the administration of the compound, thus coinciding with the exponential growth phase where bacterial metabolic activity is most active. The metabolome was sampled at intervals of 90 min to account for *S. aureus* doubling time. At later time points, the bacteria are likely to be undergoing gross changes in metabolites due to cell death. The earlier time points are more likely to be representative of the specific mechanism of action.

The metabolome extraction protocol was adapted from that described by Vincent et al.,[17] by including bead beating alongside chemical extraction (with 1:3:1 chloroform−methanol−water as the solvent) to obtain the internal metabolome.[43] Glass beads were used as previously described[43−46] for the extraction of metabolites from *S. aureus*.

Metabolome samples were analyzed by Glasgow Polyomics, University of Glasgow. The levels of metabolites and the identification of metabolites were determined based on the methods by Vincent et al.[17] The comparison of metabolite

DOI: 10.1021/acsomega.9b02507
ACS Omega 2019, 4, 19199−19215

levels was initially performed using principal component analysis (PCA). A PCA plot is useful to reduce multidimensional data such as the data gathered in this study, as each data point consists of the various intensities of metabolites detected in each sample. By reducing multidimensional data to two- or three-dimensional data, a PCA plot presents a clear visual representation to identify any clustering of data, which gives an indication of similarity with one another. Figure 5 shows the effect of various compounds exhibiting antibacterial activity on the bacterial metabolome, visualized using PCA plots.

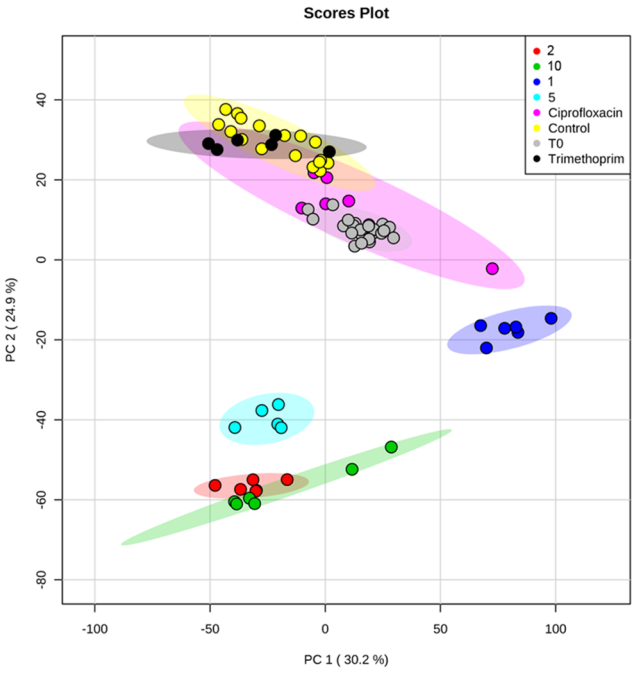

Figure 5. PCA plot of drug treatments on *S. aureus* RN6390. Raw intensities were glog transformed and the plot was generated using the MetaboAnalyst software.[47] Time points are combined for clarity and one outlier from the treatment group **5** was removed as it had much lower intensities across the entire spectrum.

Ciprofloxacin has previously been shown to cause drastic changes to the nucleotide pool,[46] and we also noted similar changes, in particular, in cytidine and guanine pool (Table S2). Trimethoprim inhibits dihydrofolate reductase (DHFR), but the folate pool was of insufficient abundance to be identified in the liquid chromatography−mass spectrometry platform we used. A significant increase in uridine is likely related to an accumulation of deoxyuridine monophosphate as its methylation to deoxythymidine monophosphate (not identified) is prevented as DHFR is inhibited depriving the cells of the key methyl group donor used in DNA synthesis.

The observation that **2** and its two analogues have distinct clusters from the rest suggests that these compounds have the same/similar mode of action. However, although changes of metabolites were observed upon treatment with **2** and its two analogues, no metabolic pathways stood out as specific targets for these compounds based on clear changes in abundance across a single enzyme. This could indicate that **2** and its analogues act against a target, which has pleiotropic effects, against several targets, or the compound could act against targets with metabolites poorly represented in the database.

As ciprofloxacin and trimethoprim target nucleic acid metabolism (DNA and folate biosynthesis, respectively), it was interesting to observe that this general similarity in their mode of action translated to similar clustering in the PCA plot in Figure 5. Based on these clustering patterns, it can be suggested that the modes of action of **2** and its analogues are distinct compared to ciprofloxacin and trimethoprim. In addition, the clustering also suggests that compound **1** may have a distinct mode of action from the rest of the compounds tested. Nevertheless, the results from these early metabolomics studies must be supported by other orthogonal biological studies to generate or further strengthen a hypothesis on the mode of action.

These early results presented the challenge of determining the right moment in an early antibacterial drug discovery program for these compounds to be subjected to metabolomics study. As these compounds (excluding marketed antibiotics) are small polar molecules with low potency, there is always the possibility of their exerting activity at multiple targets across bacterial metabolism. In this case, during hit expansion to improve the potency of the analogues, the mode of action can shift. As seen in Figure 5, the more potent compound **5** seems to have a different metabolic fingerprint from its original hit **2**. This may indicate that metabolomics can be useful to monitor whether SAR exploration may lead to a switch in the mechanism of action.

CONCLUSIONS

We have introduced the notion of small polar molecules as an attractive starting point in antibacterial drug discovery. This requires a well-constructed library to provide new chemical scaffolds with good physicochemical properties and novelty to allow efficient chemical expansion and optimization.

The whole cell screening process was designed to be amenable to high-throughput conditions, with straightforward set-up and easy-to-measure end points. From our in-house whole cell screening assay using our small polar library, we have identified two promising hit compounds, **1** and **2**. The hit expansion of **2** has been illustrated in detail in this article, with diverse chemistry to probe the effect of various substitutions on the pyrazoloylpyrimidine core. This diverse chemistry can be amenable to parallel combinatorial chemistry to allow quick synthesis of analogues as well. Some initial SAR can be observed from these analogues synthesized, with compounds such as **5** and **10** gaining potency from the original hit. Although the original low-molecular-weight hit had relatively weak activity (but good ligand efficiency), it was possible to optimize it to a compound with much greater potency, not much less potent than trimethoprim, a clinically used antibiotic. As such, we believe that this series has the potential for further rounds of chemical optimization to improve potency and physicochemical properties, using ligand efficiency metrics as indicators. As physicochemical properties of these compounds are important in ensuring not only optimal entry into the bacteria but also pharmacokinetic properties, we would suggest using ligand efficiency metrics such as LEI and LLE to guide the direction of the chemical optimization.

Early metabolomics study indicated that **2** and its analogues, alongside the other whole cell hit **1**, have distinct mode of actions compared to other antibiotics tested (ciprofloxacin and trimethoprim), even though the mode of actions for **2** and its analogues (alongside **1**) cannot be precisely determined. It is also interesting to note the shift in the mode of action as the compound is optimized. This is perhaps not surprising. A

DOI: 10.1021/acsomega.9b02507
ACS Omega 2019, 4, 19199−19215

weak, although ligand efficient, low-molecular-weight compound may inhibit several targets weakly. However, during compound optimization, the profile of which molecular targets is inhibited and by how much, may change.

Determining the precise mode of action of a molecular target can be very challenging. A future study to derive the metabolomic fingerprint of key antibiotics will be important as a reference to compare to new compounds would be very valuable. Orthogonal mode of action studies such as chemical proteomics or resistance generation followed by whole genome sequencing can also be proposed to support any hypothesis from this untargeted metabolomics approach.

Despite the limitations discussed, we are optimistic that whole cell screening coupled with metabolomic can be an attractive route to finding new starting points with novel modes of action in early antibacterial drug discovery. The work of Pogliano has shown that there is a distinct phenotype associated with compounds, which target particular pathways within bacteria.[48] There is a scope for extending this current work, by seeing if there is a correlation between the metabolome fingerprint and the morphological effect on the bacteria. This whole cell-based platform highlights the capability for finding new hits with cellular activity and potential new mode of action. The mode of action can then be validated at the early stages of hit discovery, which then increases the odds of success for the drug development process.

EXPERIMENTAL SECTION

Whole Cell Screening. The whole cell screening was performed using the in-house small polar library. The composition of the library and some illustrated examples of synthesis of such molecules were described by Ray et al.[22] Compounds from the library were stamped into each well from column 1 to column 22 of 384-well plates with a Echo 550 Liquid Handler (Labcyte Inc.). *S. aureus* RN4220 (Division of Molecular Microbiology, University of Dundee) was used for whole cell screening. All cultures, which require shaking, were shaken at 200 rpm. An overnight culture was prepared by culturing a colony in 3 mL (for *S. aureus* RN4220) of fresh LB media (Central Technical Services, University of Dundee) at 37 °C for 12−15 h. The culture was dispensed into white-walled, clear flat-bottom 384-well plates (Greiner Bio-One) by a Multidrop Combi Reagent Dispenser (Thermo Scientific). Plates were read using PHERAstar FS (BMG LABTECH). 50 μL of the culture (prepared by diluting an overnight culture of *S. aureus* RN4220 with fresh LB media at 1:400 ratio) was added to columns of each well, depending on the type of study: single-point study (columns 1−22 of the plate) or (columns 1−10 and 13−22 of the plate). The positive control (gentamicin 0.5 mg/mL) was filled into column 23 (for single-point study) or columns 11 and 23 (for dose−response study), while the negative control (no drug) was filled in the remaining columns. The plates were sealed with air-permeable seals (AeraSeal, Excel Scientific, Inc.) and incubated still at 37 °C for 6 h. The plate was then put into a plate reader to measure OD_{600nm}. All calculations were performed on ActivityBase XE (IDBS) using the raw data obtained from the plate reader. The raw data correspond to the OD_{600nm} measured on each well. PA positive control is defined as a completely active compound with 100% inhibitory effect against bacteria. The negative control is defined as a completely inactive compound with 0% inhibitory effect against bacteria. Hit analysis was performed and visualized using Vortex (Dotmatics Limited). Graphic visualization and statistical analysis were performed and visualized using Vortex and GraphPad Prism 6 (GraphPad Software Inc.).

Chemistry. *General Procedures.* Chemicals and solvents were purchased from Aldrich Chemical Co., Acros, TCI, and Fluorochem. Analytical thin-layer chromatography (TLC) was performed on precoated TLC plates (layer 0.20 mm silica gel 60 with fluorescent indicator UV 254, from Merck). Developed plates were air-dried and analyzed under a UV lamp (UV 254/365 nm) or sprayed with a potassium permanganate solution to visualize oxidizable substances. Flash column chromatography was performed using prepacked silica gel cartridges (Teledyne ISCO) using CombiFlash Rf200i (Teledyne ISCO). Microwave-assisted chemistry was conducted using a Biotage initiator microwave synthesizer. ^{1}H and ^{13}C NMR spectra were recorded on a Bruker ARX-500 spectrometer (500, 470, and 125 MHz for ^{1}H, ^{19}F, and ^{13}C NMR, respectively). Spectra were acquired using DMSO-d_6, D_2O, and $CDCl_3$ as solvents. Chemical shifts (δ) are reported in parts per million relative to the residual solvent peak as the internal reference, and coupling constants (J) are reported in hertz (Hz). Coupling constants are assumed to be H−H coupling constants unless stated otherwise. The spin multiplicity is reported as s = singlet, s(b) = broad singlet, d = doublet, t = triplet, q = quartet, m = multiplet. LC−MS analyses were performed with either an Agilent HPLC 1100 series connected to a Bruker Daltonics MicrOTOF or an Agilent Technologies 1200 series HPLC connected to an Agilent Technologies 6130 quadrupole spectrometer, where both instruments were connected to an Agilent diode array detector. LC−MS chromatographic separations were conducted with a Waters X bridge C18 column, 50 mm × 2.1 mm, 3.5 μm particle size; mobile phase, H_2O/MeCN + 0.1% HCOOH, or H_2O/MeCN + 0.1% NH_3; linear gradient from 80:20 to 5:95 over 3.5 min and then held for 1.5 min; flow rate of 0.5 mL/min. High-resolution electrospray measurements were performed on a Bruker Daltonics MicrOTOF mass spectrometer. All assay compounds had a measured purity of ≥95% (by TLC and UV) as determined using both LC−MS and NMR spectroscopy. Melting points were determined on the Griffin melting point apparatus and were uncorrected.

*General Procedure A for the Coupling of Chloropyrimidines and 3,5-Dimethylpyrazoles. Method 1 (Compounds **3**, **4**, and **17**).* To a solution of appropriate chloropyrimidine (1 equiv) in dioxane (0.2 M) was added 3,5-dimethylpyrazole (1.05 equiv) and was subjected to microwave irradiation at 150 °C for 3 h. The solvent was removed, and the crude residue was purified using flash column chromatography (DCM/heptane or EtOAc/heptane) to give the intended product.

*Method 2 (Compounds **12**−**16**).* To a solution of appropriate chloropyrimidine (1 equiv) in acetonitrile (0.33 M) were added 3,5-dimethylpyrazole (1 equiv), KOH (1 equiv), and 18-crown-6 (0.1 equiv). The reaction mixture was left to stir at rt for 1 day or was subjected to microwave irradiation at various temperatures. The reaction mixture was quenched with 2 M HCl, and the aqueous layer was extracted with ethyl acetate. The organic layer was then separated and concentrated in vacuo to give the residue, which was then purified using flash column chromatography (0−25% EtOAc in heptane) to give the intended product.

DOI: 10.1021/acsomega.9b02507
ACS Omega 2019, 4, 19199−19215

4-Chloro-2-(3,5-dimethyl-1H-pyrazol-1-yl)-6-methylpyrimidine ***(3)***. General procedure A, method 1, from 2,4-dichloro-6-methylpyrimidine (163 mg, 1.0 mmol). Chromatographic purification (50% DCM in heptane to 100% DCM) gave compound **3** as white solid (79 mg, 35%): mp: 58−60 °C (lit. mp 57 °C[49]); ^{1}H NMR ($CDCl_3$, 500 MHz) δ: 7.06 (s, 1H, Ar H), 6.07 (s, 1H, Ar H), 2.68 (s, 3H, CH_3), 2.61 (s, 3H, CH_3) 2.36 (s, 3H, CH_3). ^{13}C NMR ($CDCl_3$, 125 MHz) δ: 170.9 (C), 161.6 (C), 156.8 (C), 152.1 (C), 143.5 (C), 117.0 (CH), 110.9 (CH), 24.2 (CH_3), 15.5 (CH_3), 14.0 (CH_3); MS [electrospray ionization (ESI)] m/z 223 $[M + H]^+$ (^{35}Cl); 225 $[M + H]^+$ (^{37}Cl); high-resolution mass spectrometry (HRMS) (ESI) m/z: calcd for $C_{10}H_{12}N_4Cl^+$ $[M + H]^+$, 223.0745; found, 223.0755.

4,6-Dichloro-2-(3,5-dimethyl-1H-pyrazol-1-yl)pyrimidine ***(4)***. General procedure A, method 1, from 2,4,6-trichloropyrimidine (575 μL, 917 mg, 5.0 mmol). Chromatographic purification (50% DCM in heptane to 100% DCM) gave compound **4** as white solid (295 mg, 24%): mp 110−111 °C; ^{1}H NMR ($CDCl_3$, 500 MHz) δ: 7.21 (s, 1H, Ar H), 6.08 (s, 1H, Ar H), 2.68 (s, 3H, CH_3), 2.35 (s, 3H, CH_3); ^{13}C NMR ($CDCl_3$, 125 MHz) δ: 162.7 (2× C), 156.4 (C), 153.2 (C), 144.1 (C), 117.1 (CH), 111.8 (CH), 15.6 (CH_3), 14.0 (CH_3); MS (ESI) m/z 243 $[M + H]^+$; 245 $[M + H]^+$ (^{35}Cl^{37}Cl); 247 $[M + H]^+$ (^{37}Cl^{37}Cl); HRMS (ESI) m/z: calcd for $C_9H_9N_4Cl_2^+$ $[M + H]^+$, 243.0199; found, 243.0213.

2-(3,5-Dimethyl-1H-pyrazol-1-yl)pyrimidine ***(12)***. General procedure A, method 2, from 2-chloropyrimidine (115 mg, 1.0 mmol) and stirred at rt. Chromatographic purification gave compound **12** as brown oil (77 mg, 44%): ^{1}H NMR ($CDCl_3$, 500 MHz) δ: 8.76 (d, J = 4.8 Hz, 2H, 2× Ar H), 7.19 (t, J = 4.8 Hz, 1H), 6.07 (s, 1H, Ar H), 2.69 (s, 3H, CH_3), 2.36 (s, 3H, CH_3); ^{13}C NMR ($CDCl_3$, 125 MHz) δ: 158.4 (2× CH), 157.6 (C), 151.5 (C), 143.0 (C), 117.7 (CH), 110.3 (CH), 15.3 (CH_3), 13.8 (CH_3); MS (ESI) m/z 175 $[M + H]^+$; HRMS (ESI) m/z: calcd for $C_9H_{11}N_4^+$ $[M + H]^+$, 175.0978; found, 175.0979.

2-(3,5-Dimethyl-1H-pyrazol-1-yl)-4,6-dimethylpyrimidine ***(13)***. General procedure A, method 2, from 2-chloro-4,6-dimethylpyrimidine (143 mg, 1.0 mmol) and subjected to microwave irradiation at 80 °C for 15 min. Chromatographic purification gave compound **13** as brown oil (96 mg, 47%): ^{1}H NMR ($CDCl_3$, 500 MHz) δ: 6.90 (s, 1H, Ar H), 6.03 (s, 1H, Ar H), 2.66 (s, 3H, CH_3), 2.55 (s, 6H, 2× CH_3), 2.36 (s, 3H, CH_3); ^{13}C NMR ($CDCl_3$, 125 MHz) δ: 168.5 (C), 157.2 (C), 151.0 (C), 142.7 (C), 116.9 (CH), 109.9 (CH), 24.1 (2× CH_3), 15.2 (CH_3), 14.0 (CH_3); MS (ESI) m/z 203 $[M + H]^+$; HRMS (ESI) m/z: calcd for $C_{11}H_{14}N_4^+$ $[M + H]^+$, 203.1291; found, 203.1303.

2-(3,5-Dimethyl-1H-pyrazol-1-yl)-4-methoxypyrimidine ***(14)***. General procedure A, method 2, from 2-chloro-4-methoxypyrimidine (434 mg, 3.0 mmol) and subjected to microwave irradiation at 120 °C for 30 min. Chromatographic purification gave compound **14** as white solid (196 mg, 32%): mp 91−92 °C; ^{1}H NMR ($CDCl_3$, 500 MHz) δ: 8.49 (d, J = 5.7 Hz, 1H, Ar H), 6.59 (d, J = 5.7 Hz, 1H, Ar H), 6.06 (s, 1H, Ar H), 4.05 (s, 3H, CH_3), 2.72 (s, 3H, CH_3), 2.36 (s, 3H, CH_3); ^{13}C NMR ($CDCl_3$, 125 MHz) δ: 170.3 (C), 158.7 (CH), 157.0 (C), 151.4 (C), 142.6 (C), 110.4 (CH), 104.7 (CH), 54.3 (OCH_3), 15.6 (CH_3), 13.9 (CH_3); MS (ESI) m/z 205 $[M + H]^+$; HRMS (ESI) m/z: calcd for $C_{10}H_{13}N_4O^+$ $[M + H]^+$, 205.1084; found, 205.1097.

2-(3,5-Dimethyl-1H-pyrazol-1-yl)-4,6-dimethoxypyrimidine ***(15)***. General procedure A, method 2, from 2-chloro-4,6-dimethoxypyrimidine (524 mg, 3.0 mmol) and stirred at rt. Chromatographic purification gave compound **15** as white solid (492 mg, 70%): mp 102−104 °C; ^{1}H NMR ($CDCl_3$, 500 MHz) δ: 6.03 (s, 1H, Ar H), 5.93 (s, 1H, Ar H), 4.03 (s, 6H, 2× CH_3), 2.69 (s, 3H, CH_3), 2.34 (s, 3H, CH_3); ^{13}C NMR ($CDCl_3$, 125 MHz) δ: 172.1 (2× C), 156.1 (C), 151.3 (C), 142.8 (C), 110.3 (CH), 86.7 (CH), 54.5 (2× OCH_3), 15.6 (CH_3), 14.0 (CH_3); MS (ESI) m/z 235 $[M + H]^+$; HRMS (ESI) m/z: calcd for $C_{11}H_{15}N_4O_2^+$ $[M + H]^+$, 235.1190; found, 235.1208.

5-Chloro-2-(3,5-dimethyl-1H-pyrazol-1-yl)-4-methoxypyrimidine ***(16)***. General procedure A, method 2, from 2,5-dichloro-4-methoxypyrimidine (263 mg, 1.47 mmol) and stirred at rt. Chromatographic purification gave compound **16** as white solid (144 mg, 41%): mp 132−133 °C; ^{1}H NMR ($CDCl_3$, 500 MHz) δ: 8.50 (s, 1H, Ar H), 6.07 (s, 1H, Ar H), 4.15 (s, 3H, OCH_3), 2.70 (s, 3H, CH_3), 2.35 (s, 3H, CH_3); ^{13}C NMR ($CDCl_3$, 125 MHz) δ: 165.2 (C), 156.8 (CH), 154.7 (C), 151.9 (C), 142.7 (C), 113.2 (C), 110.7 (CH), 55.4 (CH_3), 15.5 (CH_3), 13.9 (CH_3); MS (ESI) m/z 239 $[M + H]^+$ (^{35}Cl); 227 $[M + H]^+$ (^{37}Cl); HRMS (ESI) m/z: calcd for $C_{10}H_{12}N_4OCl^+$ $[M + H]^+$, 239.0694; found, 239.0725.

Methyl 2-(3,5-Dimethyl-1H-pyrazol-1-yl)-6-methylpyrimidine-4-carboxylate ***(17)***. General procedure A, method 1, from methyl 2-chloro-6-methylpyrimidine-4-carboxylate (1.88 g, 10.1 mmol). Chromatographic purification (0−25% EtOAc in heptane) gave compound **17** as yellow solid (1.60 g, 64%): ^{1}H NMR ($CDCl_3$, 500 MHz) δ: 7.70 (s, 1H, Ar H), 6.08 (s, 1H, Ar H), 4.03 (s, 3H, OCH_3), 2.73 (s, 3H, CH_3), 2.73 (s, 3H, CH_3), 2.37 (s, 3H, CH_3); ^{13}C NMR ($CDCl_3$, 125 MHz) δ: 171.5 (C), 164.0 (C), 156.9 (C), 155.1 (C), 151.3 (C), 142.8 (C), 116.2 (CH), 110.0 (CH), 52.6 (CH_3), 24.1 (CH_3), 14.7 (CH_3), 13.4 (CH_3); MS (ESI) m/z 247 $[M + H]^+$; HRMS (ESI) m/z: calcd for $C_{12}H_{15}N_4O_2^+$ $[M + H]^+$, 247.1190; found, 247.1215.

2-(3,5-Dimethyl-1H-pyrazol-1-yl)-6-methylpyrimidin-4-ol ***(2)***. To a solution of 4,6-dichloro-2-(3,5-dimethyl-1*H*-pyrazol-1-yl)pyrimidine (**3**) (179 mg, 0.80 mmol) in THF (4 mL) was added 1 M NaOH (4 mL) and then subjected to microwave irradiation at 150 °C for 30 min. Excess base was neutralized with 2 M HCl, and the reaction mixture was extracted with ethyl acetate. The organic phase was separated and concentrated in vacuo. The residue was then purified using flash column chromatography (0−3% MeOH in DCM) to give **3** as a white solid (148 mg, 90%): mp 126−126 °C (lit. mp 135−137 °C[49]); ^{1}H NMR ($CDCl_3$, 500 MHz) δ: 10.40 (s(b), 1H, OH), 6.08 (s, 1H, Ar H), 6.05 (s, 1H, Ar H), 2.69 (s, 3H, CH_3), 2.30 (s, 3H, CH_3), 2.27 (s, 3H, CH_3); ^{13}C NMR ($CDCl_3$, 125 MHz) δ: 165.1 (C), 161.9 (C), 151.9 (C), 147.5 (C), 143.6 (C), 111.5 (CH), 108.9 (CH), 24.0 (CH_3), 15.1 (CH_3), 13.6 (CH_3); MS (ESI) m/z 205 $[M + H]^+$; HRMS (ESI) m/z: calcd for $C_{10}H_{13}N_4O^+$ $[M + H]^+$, 205.1084; found, 205.1091.

Alternative Procedure Using TFA−DCM. To 2-(3,5-dimethyl-1*H*-pyrazol-1-yl)-4-((4-methoxybenzyl)oxy)-6-methylpyrimidine (**5**) (49 mg, 0.15 mmol) was added excess volume of trifluoroacetic acid (200 equiv) and an equivalent volume of DCM. The reaction mixture was left to stir for 1 h at rt. The reaction mixture was evaporated in vacuo, and the residue was purified by reverse-phase UV-HPLC to give **2** as a white solid (22 mg, 72%).

DOI: 10.1021/acsomega.9b02507
ACS Omega 2019, 4, 19199−19215

*6-Chloro-2-(3,5-dimethyl-1H-pyrazol-1-yl)pyrimidin-4-ol (**10**).* To a solution of 4,6-dichloro-2-(3,5-dimethyl-1*H*-pyrazol-1-yl)pyrimidine (**4**) (100 mg, 0.41 mmol) in THF (2.05 mL) were added 1 M NaOH (0.82 mL) and additional water (1.23 mL) and then subjected to microwave irradiation at 150 °C for 30 min. Excess base was neutralized with 2 M HCl, and the reaction mixture was extracted with ethyl acetate. The organic phase was separated and concentrated in vacuo. The residue was then purified using flash column chromatography (DCM) to give **10** as a white solid (63 mg, 68%): mp 132−134 °C; ^{1}H NMR ($CDCl_3$, 500 MHz) δ: 10.50 (s(b), 1H, OH), 6.29 (s, 1H, Ar H), 6.04 (s, 1H, Ar H), 2.69 (s, 3H, CH_3), 2.28 (s, 3H, CH_3); ^{13}C NMR ($CDCl_3$, 125 MHz) δ: 160.4 (C), 158.8 (C), 153.2 (C), 147.4 (C), 144.3 (C), 112.3 (CH), 109.3 (CH), 15.0 (CH_3), 13.6 (CH_3); MS (ESI) m/z 225 $[M + H]^+$ (^{35}Cl); 227 $[M + H]^+$ (^{37}Cl); HRMS (ESI) m/z: calcd for $C_9H_{10}N_4ClO^+$ $[M + H]^+$, 225.0538; found, 225.0497.

*General Procedure B for the Formation of Benzyl Ether Analogues (Compounds **5**−**9**).* To a solution of 4-chloro-2-(3,5-dimethyl-1*H*-pyrazol-1-yl)-6-methylpyrimidine (**3**) (1 equiv) in acetonitrile (0.3 M) were added the appropriate benzyl alcohol (1.2 equiv) and Cs_2CO_3 (1.2 equiv). The reaction mixture was then refluxed overnight. The reaction mixture was then cooled to rt and diluted with ethyl acetate. The organic phase was then washed with brine, dried, and concentrated in vacuo. The crude product was then purified using flash column chromatography (0−50% ethyl acetate in heptane) to give the desired product.

*2-(3,5-Dimethyl-1H-pyrazol-1-yl)-4-((4-methoxybenzyl)-oxy)-6-methylpyrimidine (**5**).* General procedure B, from 4-methoxybenzyl alcohol (350 mg, 2.53 mmol) to give **5** as white solid (542 mg, 79%): mp 58−60 °C; ^{1}H NMR ($CDCl_3$, 500 MHz) δ: 7.37 (d, J = 8.7 Hz, 2H, 2× Ar H), 6.93 (d, J = 8.7 Hz, 2H, 2× Ar H), 6.48 (s, 1H, Ar H), 6.04 (s, 1H, Ar H), 5.39 (s, 2H, CH_2), 3.84 (s, 3H, OCH_3), 2.69 (s, 3H, CH_3), 2.54 (s, 3H, CH_3), 2.36 (s, 3H, CH_3); ^{13}C NMR ($CDCl_3$, 125 MHz) δ: 170.1 (C), 169.6 (C), 159.7 (C), 156.6 (C), 151.2 (C), 142.5 (C), 129.8 (2× CH), 128.0 (C), 114.1 (2× CH), 110.2 (CH), 103.6 (CH), 68.4 (CH_2), 55.3 (CH_3), 24.3 (CH_3), 15.5 (CH_3), 14.0 (CH_3); MS (ESI) m/z 325 $[M + H]^+$; HRMS (ESI) m/z: calcd for $C_{18}H_{21}N_4O_2^+$ $[M + H]^+$, 325.1659; found, 325.1685.

*2-(3,5-Dimethyl-1H-pyrazol-1-yl)-4-((3-methoxybenzyl)-oxy)-6-methylpyrimidine (**6**).* General procedure B, from 3-methoxybenzyl alcohol alcohol (67 μL, 74 mg, 0.54 mmol) to give **6** as white solid (52 mg, 36%): ^{1}H NMR ($CDCl_3$, 500 MHz) δ: 7.23 (dd, J_1 = 7.9 Hz, J_2 = 7.9 Hz, 1H, Ar H), 6.93−6.90 (m, 1H, Ar H), 6.90−6.88 (m, 1H, Ar H), 6.82−6.79 (m, 1H, Ar H), 6.43 (s, 1H, Ar H), 5.94 (s, 1H, Ar H), 5.34 (s, 2H, CH_2), 3.74 (s, 3H, OCH_3), 2.56 (s, 3H, CH_3), 2.47 (s, 3H, CH_3), 2.27 (s, 3H, CH_3); ^{13}C NMR ($CDCl_3$, 125 MHz) δ: 170.1 (C), 169.8 (C), 159.8 (C), 156.6 (C), 151.2 (C), 142.6 (C), 137.5 (C), 129.7 (CH), 120.0 (CH), 113.7 (CH), 113.4 (CH), 110.2 (CH), 103.6 (CH), 68.4 (CH_2), 55.3 (CH_3), 24.3 (CH_3), 15.5 (CH_3), 14.0 (CH_3); MS (ESI) m/z 325 $[M + H]^+$; HRMS (ESI) m/z: calcd for $C_{18}H_{21}N_4O_2^+$ $[M + H]^+$, 325.1659; found, 325.1610.

*2-(3,5-Dimethyl-1H-pyrazol-1-yl)-4-((2-methoxybenzyl)-oxy)-6-methylpyrimidine (**7**).* General procedure B, from 2-methoxybenzyl alcohol (72 μL, 74 mg, 0.54 mmol) to give **7** as white solid (55 mg, 38%): ^{1}H NMR ($CDCl_3$, 500 MHz) δ: 7.39−7.38 (m, 1H, Ar H), 7.34 (td, J_1 = 7.9 Hz, J_2 = 1.6 Hz, 1H, Ar H), 6.98 (td, J_1 = 7.5 Hz, J_2 = 1.0 Hz, 1H, Ar H), 6.93−6.95 (m, 1H, Ar H), 6.52 (s, 1H, Ar H), 6.02 (s, 1H, Ar H), 5.50 (s, 2H, CH_2), 3.87 (s, 3H, OCH_3), 2.63 (s, 3H, CH_3), 2.56 (s, 3H, CH_3), 2.36 (s, 3H, CH_3); ^{13}C NMR ($CDCl_3$, 125 MHz) δ: 170.2 (C), 169.6 (C), 157.4 (C), 156.6 (C), 151.1 (C), 142.7 (C), 129.5 (CH), 129.2 (CH), 124.3 (C), 120.5 (CH), 110.4 (CH), 110.1 (CH), 103.5 (CH), 64.1 (CH_2), 55.4 (CH_3), 24.3 (CH_3), 15.3 (CH_3), 14.0 (CH_3); MS (ESI) m/z 325 $[M + H]^+$; HRMS (ESI) m/z: calcd for $C_{18}H_{21}N_4O_2^+$ $[M + H]^+$, 325.1659; found, 325.1599.

*2-(3,5-Dimethyl-1H-pyrazol-1-yl)-4-((4-fluorobenzyl)oxy)-6-methylpyrimidine (**8**).* General procedure B, from 4-fluorobenzyl alcohol (70 μL, 82 mg, 0.65 mmol) to give **8** as white solid (132 mg, 78%): ^{1}H NMR ($CDCl_3$, 500 MHz) δ: 7.33 (dd, $^3J_{HH}$ = 8.8 Hz, $^4J_{HF}$ = 5.4 Hz, 2H, 2× Ar H), 7.00 (dd, $^3J_{HH}$ = 8.7 Hz, $^3J_{HF}$ = 8.7 Hz, 2H, 2× Ar H), 6.41 (s, 1H, Ar H), 5.95 (s, 1H, Ar H), 5.33 (s, 2H, CH_2), 2.57 (s, 3H, CH_3), 2.46 (s, 3H, CH_3), 2.27 (s, 3H, CH_3); ^{13}C NMR ($CDCl_3$, 125 MHz) δ: 170.0 (C), 169.8 (C), 162.7 (d, $^1J_{CF}$ = 247.2 Hz, C), 156.5 (C), 151.3 (C), 142.5 (C), 131.8 (C), 129.9 (d, $^3J_{CF}$ = 8.2 Hz, 2× CH), 115.6 (d, $^2J_{CF}$ = 21.7 Hz, 2× CH), 110.3 (CH), 103.5 (CH), 67.8 (CH_2), 24.3 (CH_3), 15.5 (CH_3), 14.0 (CH_3); ^{19}F NMR ($CDCl_3$, 470 MHz) δ: −113.6 (Ar F); MS (ESI) m/z 313 $[M + H]^+$; HRMS (ESI) m/z: calcd for $C_{17}H_{18}FN_4O^+$ $[M + H]^+$, 313.1459; found, 313.1393.

*4-(Benzyloxy)-2-(3,5-dimethyl-1H-pyrazol-1-yl)-6-methyl-pyrimidine (**9**).* General procedure B, from benzyl alcohol (56 μL, 58 mg, 0.54 mmol) to give **9** as white solid (71 mg, 54%): ^{1}H NMR ($CDCl_3$, 500 MHz) δ: 7.45−7.35 (m, 5H, 5× Ar H), 6.52 (s, 1H, Ar H), 6.04 (s, 1H, Ar H), 5.47 (s, 2H, CH_2), 2.66 (s, 3H, CH_3), 2.56 (s, 3H, CH_3), 2.36 (s, 3H, CH_3); ^{13}C NMR ($CDCl_3$, 125 MHz) δ: 170.1 (C), 169.8 (C), 156.6 (C), 151.3 (C), 142.6 (C), 136.0 (C), 128.6 (2× CH), 128.3 (CH), 127.9 (2× CH), 110.2 (CH), 103.6 (CH), 68.5 (CH_2), 24.3 (CH_3), 15.5 (CH_3), 14.0 (CH_3); MS (ESI) m/z 295 $[M + H]^+$; HRMS (ESI) m/z: calcd for $C_{17}H_{19}N_4O^+$ $[M + H]^+$, 295.1553; found, 295.1553.

*2-(3,5-Dimethyl-1H-pyrazol-1-yl)-3,6-dimethylpyrimidin-4(3H)-one (**11**).* To a solution of 2-(3,5-dimethyl-1*H*-pyrazol-1-yl)-6-methylpyrimidin-4-ol (**2**) (51 mg, 0.25 mmol) and K_2CO_3 (69 mg, 0.50 mmol) in DMF (2.77 mL) was added methyl iodide (62 μL, 1.00 mmol). The reaction was then refluxed overnight. Water was added into the reaction mixture, and the reaction mixture was washed with ethyl acetate. The organic phase was then separated, dried, and concentrated in vacuo to give a residue, which was purified using flash column chromatography (10−25% ethyl acetate in heptane) to give **11** as a off-brown solid (41 mg, 75%): ^{1}H NMR ($CDCl_3$, 500 MHz) δ: 6.24 (s, 1H, Ar H), 5.94 (s, 1H, Ar H), 3.34 (s, 3H, NCH_3), 2.28 (s, 3H, CH_3), 2.22 (s, 3H, CH_3), 2.20 (s, 3H, CH_3); ^{13}C NMR ($CDCl_3$, 125 MHz) δ: 163.1 (C), 162.1 (C), 151.5 (C), 148.3 (C), 142.4 (C), 111.4 (CH), 108.1 (CH), 32.2 (CH_3), 23.4 (CH_3), 13.6 (CH_3), 11.8 (CH_3); MS (ESI) m/z 219 $[M + H]^+$; HRMS (ESI) m/z: calcd for $C_{11}H_{15}N_4O^+$ $[M + H]^+$, 219.1240; found, 219.1243.

*2-(3,5-Dimethyl-1H-pyrazol-1-yl)-6-methylpyrimidine-4-carboxylic Acid (**18**).* To a solution of methyl 2-(3,5-dimethyl-1*H*-pyrazol-1-yl)-6-methylpyrimidine-4-carboxylate (**17**) (231 mg, 0.94 mmol) in 1:1 THF/H_2O (14 mL) was added lithium hydroxide (79 mg, 1.88 mmol), and the reaction mixture was allowed to stir overnight at rt. The reaction mixture was concentrated in vacuo, and the residue was purified using mass-directed HPLC to give **18** as a white solid (190 mg,

DOI: 10.1021/acsomega.9b02507
ACS Omega 2019, 4, 19199−19215

87%): ^{1}H NMR ($CDCl_3$, 500 MHz) δ: 7.82 (s, 1H, Ar H), 7.07 (s(b), 1H, OH), 6.10 (s, 1H, Ar H), 2.74 (s, 3H, CH_3), 2.70 (s, 3H, CH_3), 2.35 (s, 3H, CH_3); ^{13}C NMR ($CDCl_3$, 125 MHz) δ: 172.3 (C), 164.3 (C), 156.5 (C), 155.5 (C), 152.0 (C), 143.7 (C), 116.2 (CH), 111.0 (CH), 24.6 (CH_3), 15.6 (CH_3), 13.6 (CH_3); MS (ESI) m/z 233 $[M + H]^+$; HRMS (ESI) m/z: calcd for $C_{11}H_{14}N_4O_2^+$ $[M + H]^+$, 233.1033; found, 233.1056.

*General Procedure C for the O-Demethylation of Methoxypyrimidines Using LiCl (Compounds **19**–**22**).* To a solution of the suitable methoxypyrimidines (1 equiv) in DMF (0.2 M) was added LiCl (3 equiv unless otherwise stated). The reaction mixture was subjected to microwave irradiation at 160 °C for 30 min (unless otherwise stated). The reaction was then acidified with dilute HCl. The aqueous layer was then extracted with DCM. The organic phase was then collected and concentrated in vacuo to give the residue, which was purified using UV-directed HPLC to yield the appropriate product.

*2-(3,5-Dimethyl-1H-pyrazol-1-yl)pyrimidin-4-ol (**19**).* General procedure C, from 2-(3,5-dimethyl-1*H*-pyrazol-1-yl)-4-methoxypyrimidine (**14**) (41 mg, 0.20 mmol) to give **19** as off-brown solid (37 mg, 97%): mp 99–100 °C; ^{1}H NMR ($CDCl_3$, 500 MHz) δ: 10.56, (s(b), 1H, OH), 7.84 (d, J = 6.7 Hz, 1H, Ar H), 6.24 (d, J = 6.6 Hz, 1H, Ar H), 6.07 (s, 1H, Ar H), 2.68 (s, 3H, CH_3), 2.28 (s, 3H, CH_3); ^{13}C NMR ($CDCl_3$, 125 MHz) δ: 161.2 (C), 154.1 (CH), 152.2 (C), 143.7 (C), 111.9 (CH), 111.7 (CH), 15.0 (CH_3), 13.6 (CH_3); MS (ESI) m/z 191 $[M + H]^+$; HRMS (ESI) m/z: calcd for $C_9H_{11}N_4O^+$ $[M + H]^+$, 191.0927; found, 191.0928.

*2-(3,5-Dimethyl-1H-pyrazol-1-yl)-6-methoxypyrimidin-4-ol (**20**).* General procedure C, from 2-(3,5-dimethyl-1*H*-pyrazol-1-yl)-4,6-dimethoxypyrimidine (**15**) (47 mg, 0.20 mmol) to give **20** as white solid (38 mg, 86%): mp 189–191 °C; ^{1}H NMR ($CDCl_3$, 500 MHz) δ: 10.20 (s(b), 1H, OH), 5.99 (s, 1H, Ar H), 5.42 (s, 1H, Ar H), 3.83 (s, 3H, OCH_3), 2.61 (s, 3H, CH_3), 2.18 (s, 3H, CH_3); ^{13}C NMR ($CDCl_3$, 125 MHz) δ: 170.6 (C), 163.1 (C), 152.7 (C), 147.9 (C), 143.5 (C), 111.9 (CH), 87.4 (CH), 55.1 (CH_3), 15.1 (CH_3), 13.6 (CH_3); MS (ESI) m/z 222 $[M + H]^+$; HRMS (ESI) m/z: calcd for $C_{10}H_{13}N_4O_2^+$ $[M + H]^+$, 221.1033; found, 221.1043.

*2-(3,5-Dimethyl-1H-pyrazol-1-yl)pyrimidine-4,6-diol (**21**).* General procedure C, from 2-(3,5-dimethyl-1*H*-pyrazol-1-yl)-4,6-dimethoxypyrimidine (**15**) (47 mg, 0.20 mmol) with 6 equiv of LiCl and microwave irradiation at 160 °C for 3 h to give **21** as white solid (10 mg, 24%): mp 197–199 °C; ^{1}H NMR ($CDCl_3$, 500 MHz) δ: 6.06 (s, 1H, Ar H), 5.58 (s, 1H, Ar H), 2.66 (s, 3H, CH_3), 2.26 (s, 3H, CH_3); ^{13}C NMR ($CDCl_3$, 125 MHz) δ: 152.8 (C), 148.0 (C), 143.8 (C), 112.0 (CH), 87.2 (CH), 15.0 (CH_3), 13.6 (CH_3); MS (ESI) m/z 207 $[M + H]^+$; HRMS (ESI) m/z: calcd for $C_9H_{21}N_4O_2^+$ $[M + H]^+$, 207.0877; found, 207.0878.

*5-Chloro-2-(3,5-dimethyl-1H-pyrazol-1-yl)pyrimidin-4-ol (**22**).* General procedure C, from 5-chloro-2-(3,5-dimethyl-1*H*-pyrazol-1-yl)-4-methoxypyrimidine (**16**) (33 mg, 0.14 mmol) to give **22** as white solid (38 mg, 86%): mp 151–152 °C; ^{1}H NMR ($CDCl_3$, 500 MHz) δ: 10.76 (s(b), 1H, OH), 8.00 (s, 1H, Ar H), 6.08 (s, 1H, Ar H), 2.66 (s, 3H, CH_3), 2.27 (s, 3H, CH_3); ^{13}C NMR ($CDCl_3$, 125 MHz) δ: 157.3 (C), 152.6 (CH), 151.0 (C), 147.0 (C), 143.8 (C), 119.3 (C), 112.0 (CH), 14.9 (CH_3), 13.6 (CH_3); MS (ESI) m/z 225 $[M + H]^+$ (^{35}Cl); 227 $[M + H]^+$ (^{37}Cl); HRMS (ESI) m/z: calcd for $C_9H_{10}N_4OCl^+$ $[M + H]^+$, 225.0538; found, 225.0536.

*General Procedure D for the Formation of Substituted Amides (Compounds **23**–**25**).* Methyl 2-(3,5-dimethyl-1*H*-pyrazol-1-yl)-6-methylpyrimidine-4-carboxylate (**17**) (1 equiv) was dissolved in suitable amines (5 equiv) in methanol, and the reaction mixture was left to stir overnight at rt. The reaction mixture was concentrated in vacuo to give the intended product.

*2-(3,5-Dimethyl-1H-pyrazol-1-yl)-6-methylpyrimidine-4-carboxamide (**23**).* General procedure D, using 7 M NH_3 in methanol (1.54 mL) to give **23** as off-yellow solid (493 mg, 99%): ^{1}H NMR ($CDCl_3$, 500 MHz) δ: 7.85 (s, 1H, Ar H), 7.79 (s(b), 1H, NH), 6.10 (s, 1H, Ar H), 6.00 (s(b), 1H, NH), 2.72 (s, 3H, CH_3), 2.70 (s, 3H, CH_3), 2.37 (s, 3H, CH_3); ^{13}C NMR ($CDCl_3$, 125 MHz) δ: 172.4 (C), 164.9 (C), 157.1 (C), 156.6 (C), 151.9 (C), 142.7 (C), 115.0 (CH), 110.8 (CH), 24.8 (CH_3), 15.5 (CH_3), 13.9 (CH_3); MS (ESI) m/z 232 $[M + H]^+$; HRMS (ESI) m/z: calcd for $C_{11}H_{14}N_5O^+$ $[M + H]^+$, 232.1193; found, 232.1212.

*2-(3,5-Dimethyl-1H-pyrazol-1-yl)-N,6-dimethylpyrimidine-4-carboxamide (**24**).* General procedure D, using 2 M methylamine in methanol (1.29 mL) to give **24** as yellow solid (126 mg, 100%): ^{1}H NMR ($CDCl_3$, 500 MHz) δ: 8.24 (s(b), 1H, NH), 7.84 (s, 1H, Ar H), 6.09 (s, 1H, Ar H), 3.06 (d, J = 5.1 Hz, 3H, NCH_3), 2.70 (s, 3H, CH_3), 2.69 (s, 3H, CH_3), 2.37 (s, 3H, CH_3); ^{13}C NMR ($CDCl_3$, 125 MHz) δ: 171.9 (C), 163.3 (C), 157.9 (C), 156.4 (C), 151.7 (C), 143.0 (C), 114.7 (CH), 110.6 (CH), 26.3 (CH_3), 24.6 (CH_3), 15.5 (CH_3), 13.8 (CH_3); MS (ESI) m/z 246 $[M + H]^+$; HRMS (ESI) m/z: calcd for $C_{12}H_{16}N_5O^+$ $[M + H]^+$, 246.1349; found, 246.1374.

*2-(3,5-Dimethyl-1H-pyrazol-1-yl)-N,N,6-trimethylpyrimidine-4-carboxamide (**25**).* General procedure D, using 2 M dimethylamine in methanol (1.34 mL) to give **25** as off-yellow solid (138 mg, 99%): ^{1}H NMR ($CDCl_3$, 500 MHz) δ: 7.18 (s, 1H, Ar H), 5.97 (s, 1H, Ar H), 3.06 (s, 3H, NCH_3), 3.02 (s, 3H, NCH_3), 2.58 (s, 3H, CH_3), 2.56 (s, 3H, CH_3), 2.27 (s, 3H, CH_3); ^{13}C NMR ($CDCl_3$, 125 MHz) δ: 171.3 (C), 166.7 (C), 162.3 (C), 156.4 (C), 151.7 (C), 143.0 (C), 116.0 (CH), 110.5 (CH), 38.7 (CH_3), 35.5 (CH_3), 24.7 (CH_3), 15.4 (CH_3), 14.0 (CH_3); MS (ESI) m/z 260 $[M + H]^+$; HRMS (ESI) m/z: calcd for $C_{13}H_{18}N_5O^+$ $[M + H]^+$, 260.1506; found, 260.1510.

*2-(3,5-Dimethyl-1H-pyrazol-1-yl)-6-methylpyrimidine-4-carbonitrile (**26**).* To a solution of 2-(3,5-dimethyl-1*H*-pyrazol-1-yl)-6-methylpyrimidine-4-carboxamide (**23**) (50 mg, 0.22 mmol) in THF (1 mL) was added Burgess reagent (258 mg, 1.08 mmol) in two portions, and the reaction mixture was allowed to stir overnight at rt. Water was added to the reaction, and the reaction mixture was washed with DCM. The organic phase was separated, dried, and concentrated in vacuo to give a residue, which was purified using flash column chromatography (0–50% ethyl acetate in heptane) to give **26** as a white solid (43 mg, 93%): ^{1}H NMR ($CDCl_3$, 500 MHz) δ: 7.34 (s, 1H, Ar H), 6.10 (s, 1H, Ar H), 2.72 (s, 3H, CH_3), 2.69 (s, 3H, CH_3), 2.37 (s, 3H, CH_3); ^{13}C NMR ($CDCl_3$, 125 MHz) δ: 172.3 (C), 157.5 (C), 152.8 (C), 143.9 (C), 141.6 (C), 120.2 (CH), 115.3 (C), 111.5 (CH), 24.7 (CH_3), 15.6 (CH_3), 14.0 (CH_3); MS (ESI) m/z 214 $[M + H]^+$; HRMS (ESI) m/z: calcd for $C_{11}H_{12}N_5^+$ $[M + H]^+$, 214.1087; found, 214.1101.

*Ethyl 2-Methyl-3-oxopropanoate (**27**).* To a stirred solution of ethyl propionate (2.30 mL, 2.04 g, 20 mmol),

DOI: 10.1021/acsomega.9b02507
ACS Omega 2019, 4, 19199–19215

methyl formate (3.70 mL, 3.60 g, 60 mmol) in DCM (20 mL) at 0 °C was added 1.0 M $TiCl_4$ solution in DCM dropwise (40 mL). After 30 min, trimethylamine (6.97 mL, 5.06 g, 50 mmol) was added dropwise. After 1 h, the reaction mixture was warmed to rt over the period of 3 h. The reaction was then quenched with water and extracted with DCM. The organic phase was then separated, dried, and concentrated in vacuo to give a residue, which was purified using flash column chromatography (DCM) to give **27** as oil with fruity odor (1.63 g, 63%). NMR spectra indicated a mixture of the aldehyde and enol tautomers with the ratio of approximately 1.5:1. ^{1}H NMR ($CDCl_3$, 500 MHz) δ: Aldehyde tautomer: 9.81 (d, J = 1.5 Hz, 1H, aldehyde H), 4.27 (q, J = 7.2 Hz, 2H, CH_2CH_3), 3.41 (qd, J_1 = 7.2 Hz, J_2 = 1.5 Hz, 1H, CH), 1.38 (d, J = 7.2 Hz, 3H, CH_3), 1.33 (t, J = 7.2 Hz, 3H, CH_2CH_3). Enol tautomer: 11.3 (d, J = 12.5 Hz, 1H, OH), 7.02 (dq, J_1 = 12.5 Hz, J_2 = 1.2 Hz, 1H, CH), 4.27 (q, J = 7.2 Hz, 2H, CH_2CH_3), 1.70 (d, J = 1.2 Hz, 3H, CH_3), 1.35 (t, J = 7.1 Hz, 3H, CH_2CH_3). ^{13}C NMR ($CDCl_3$, 125 MHz) δ: Aldehyde tautomer: 197.4 (CH), 169.7 [C, estimated from heteronuclear multiple bond correlation (HMBC)], 61.6 (CH_2), 52.7 (CH), 14.2 (CH_3), 10.3 (CH_3). Enol tautomer: 172.4 (C, estimated from HMBC), 160.1 (CH), 100.2 (C), 60.4 (CH_2), 14.2 (CH_3), 12.4 (CH_3). NMR spectra in concordance with those reported by El-Mansy et al.[50]

*General Procedure E for the Formation of Pyrazolone Derivatives (Compounds **28** and **29**).* To a solution of aminoguanidine hemisulfate (1 equiv) in water (2.5 M) were added NaOAc (1 equiv) and the appropriate β-keto ester or β-aldehydoester (1 equiv). The reaction mixture was left to stir at rt. The precipitate was then filtered and washed with minimum volume of cold water to give the intended product.

*5-Hydroxy-3-methyl-1H-pyrazole-1-carboximidamide (**28**).* General procedure E, using ethyl acetoacetate (5.46 mL, 5.61 g, 43.1 mmol) and stirred overnight to give **28** as an off-white solid (3.87 g, 64%): ^{1}H NMR (DMSO-d_6, 500 MHz) δ: 10.3 (s(b), 1H, OH), 7.72 (s(b), 3H, NH_2 and NH), 4.43 (s, 1H, Ar H), 1.97 (s, 3H, CH_3); ^{13}C NMR (DMSO-d_6, 125 MHz) δ: 168.1 (C), 156.5 (C), 153.5 (C), 82.6 (CH), 15.4 (CH_3); HRMS (ESI) m/z: calcd for $C_5H_9N_4O^+$ $[M + H]^+$, 141.0771; found, 141.0757.

*5-Hydroxy-4-methyl-1H-pyrazole-1-carboximidamide (**29**).* General procedure E, using ethyl 2-methyl-3-oxopropanoate (**27**) (381 mg, 2.93 mmol) and stirred for 7 days to give **29** as as off-white solid (214 mg, 52%): ^{1}H NMR (DMSO-d_6, 500 MHz) δ: 10.5 (s(b), 1H, OH), 7.83 (s(b), 3H, NH_2 and NH), 7.28 (s, 1H, Ar H), 1.64 (s, 3H, CH_3); ^{13}C NMR (DMSO-d_6, 125 MHz) δ: 165.8 (C), 154.0 (C), 148.5 (CH), 88.8 (C), 8.0 (CH_3); HRMS (ESI) m/z: calcd for $C_5H_9N_4O^+$ $[M + H]^+$, 141.0771; found, 141.0775.

*General Procedure F for the Formation of Carboximidamides (Compounds **32**–**34**).* To a solution of appropriate amine (1.01 equiv) in acetonitrile (2.3 M) were added triethylamine (1.01 equiv) and 1*H*-pyrazole-1-carboximidamide (1 equiv). The reaction mixture was refluxed overnight. The reaction mixture was then cooled down to rt, and the precipitate was filtered from the reaction mixture to give the product as a hydrochloride salt.

*Pyrrolidine-1-carboximidamide Hydrochloride (**32**).* General procedure F, using pyrrolidine (132 μL, 113 mg, 1.58 mmol) to give **32** as a light yellow solid (177 mg, 75%): ^{1}H NMR (DMSO-d_6, 500 MHz) δ: 7.35 (s(b), 4× NH), 3.34–3.31 (m, 4H, 2× CH_2), 1.92–1.89 (m, 4H, 2× CH_2); ^{13}C NMR (DMSO-d_6, 125 MHz) δ: 155.1 (C), 47.4 (2× CH_2), 25.2 (2× CH_2); HRMS (ESI) m/z: calcd for $C_5H_{12}N_3^+$ $[M + H]^+$, 114.1026; found, 114.1042.

*2-Methylpyrrolidine-1-carboximidamide Hydrochloride (**33**).* General procedure F, using 2-methylpyrrolidine (530 μL, 442 mg, 5.19 mmol) to give **33** as a light yellow solid (717 mg, 85%): ^{1}H NMR (DMSO-d_6, 500 MHz) δ: 7.35 (s(b), 4× NH), 4.09–4.03 (m, 1H, CH), 3.47–3.43 (m, 1H, CH from CH_2), 3.28–3.23 (m, 1H, CH from CH_2), 2.06–1.88 (m, 3H, CH_2 and CH from CH_2), 1.69–1.62 (m, 1H, CH from CH_2), 1.10 (d, J = 6.3 Hz, 3H, CH_3); ^{13}C NMR (DMSO-d_6, 125 MHz) δ: 154.6 (C), 53.9 (CH), 47.3 (CH_2), 32.5 (CH_2), 22.8 (CH_2), 19.2 (CH_3); HRMS (ESI) m/z: calcd for $C_6H_{14}N_3^+$ $[M + H]^+$, 128.1182; found, 128.1193.

*Morpholine-4-carboximidamide Hydrochloride (**34**).* General procedure F, using morpholine (451 μL, 456 mg, 5.23 mmol) to give **34** as a light yellow solid (633 mg, 74%): ^{1}H NMR (DMSO-d_6, 500 MHz) δ: 7.66 (s(b), 4× NH), 3.65–3.63 (m, 4H, 2× CH_2), 3.44–3.42 (m, 4H, 2× CH_2); ^{13}C NMR (DMSO-d_6, 125 MHz) δ: 157.1 (C), 65.7 (2× CH_2), 45.6 (2× CH_2); HRMS (ESI) m/z: calcd for $C_5H_{12}N_3O^+$ $[M + H]^+$, 130.0975; found, 130.0975.

*General Procedure G for the Ring Formation of Substituted Pyrimidines from Carboximidamides (Compounds **30**, **31**, **33**, **36**, and **37**).* To a solution of the suitable carboximidamides (1 equiv) in ethanol (0.6 M) were added NaOEt (1 equiv) and ethyl acetoacetate (1 equiv). The reaction mixture was refluxed overnight. Work-up and purification described individually in each example gave the intended product.

*2-(5-Hydroxy-3-methyl-1H-pyrazol-1-yl)-6-methylpyrimidin-4-ol (**30**).* General procedure G, from 5-hydroxy-3-methyl-1*H*-pyrazole-1-carboximidamide (**28**) (315 mg, 2.25 mmol). The precipitate was filtered and washed with a minimal volume of cold acetonitrile to give **30** as a off-red solid (174 mg, 38%): ^{1}H NMR (DMSO-d_6, 500 MHz) δ: 15.0 (s(b), 1H, OH), 5.70 (s, 1H, Ar H), 4.50 (s, 1H, Ar H), 2.13 (s, 3H, CH_3), 1.98 (s, 3H, CH_3); ^{13}C NMR (DMSO-d_6, 125 MHz) δ: 168.0 (C), 165.4 (C), 162.1 (C), 154.0 (C), 151.7 (C), 105.5 (CH), 83.0 (CH), 24.2 (CH_3), 15.4 (CH_3); MS (ESI) m/z 207 $[M + H]^+$; HRMS (ESI) m/z: calcd for $C_9H_{11}N_4O_2^+$ $[M + H]^+$, 207.0877; found, 207.0899.

*2-(5-Hydroxy-4-methyl-1H-pyrazol-1-yl)-6-methylpyrimidin-4-ol (**31**).* General procedure G, from 5-hydroxy-4-methyl-1*H*-pyrazole-1-carboximidamide (**29**) (98 mg, 0.70 mmol). The reaction mixture was concentrated in vacuo, and the residue was purified using mass-directed HPLC to give **31** as an off-yellow solid (41 mg, 28%): ^{1}H NMR ($CDCl_3$, 500 MHz) δ: 9.19 (s(b), 2H, 2× OH), 7.32 (s, 1H, Ar H), 5.98 (s, 1H, Ar H), 2.21 (s, 3H, CH_3), 1.85 (s, 3H, CH_3); ^{13}C NMR ($CDCl_3$, 125 MHz) δ: 162.4 (C), 161.3 (C), 148.8 (C), 144.8 (C), 132.5 (CH), 109.0 (CH), 98.9 (C), 23.3 (CH_3), 6.5 (CH_3); MS (ESI) m/z 207 $[M + H]^+$; HRMS (ESI) m/z: calcd for $C_9H_{11}N_4O_2^+$ $[M + H]^+$, 207.0877; found, 207.0888.

*6-Methyl-2-(pyrrolidin-1-yl)pyrimidin-4-ol (**35**).* General procedure G, from pyrrolidine-1-carboximidamide hydrochloride (**32**) (173 mg, 1.16 mmol). Water was added to the reaction, and the mixture was washed with DCM. The organic phase was then separated, dried, and concentrated in vacuo to give a residue, which was purified using flash column chromatography (0–5% MeOH/NH_3 in DCM) to give **35** as an off-white solid (133 mg, 64%): ^{1}H NMR ($CDCl_3$, 500 MHz) δ: 11.2 (s(b), 1H, OH), 5.61 (s, 1H, Ar H), 3.60–3.58

DOI: 10.1021/acsomega.9b02507
ACS Omega 2019, 4, 19199–19215

(m, 4H, 2× CH_2), 2.18 (s, 3H, CH_3), 2.03−2.00 (m, 4H, 2× CH_2); ^{13}C NMR ($CDCl_3$, 125 MHz) δ: 167.8 (C), 165.8 (C), 152.3 (C), 99.5 (CH), 46.8 (2× CH_2), 25.4 (2× CH_2), 24.5 (CH_3); MS (ESI) m/z 180 $[M + H]^+$; HRMS (ESI) m/z: calcd for $C_9H_{13}N_3O^+$ $[M + H]^+$, 180.1131; found, 180.1136.

*6-Methyl-2-(2-methylpyrrolidin-1-yl)pyrimidin-4-ol (**36**).* General procedure G, from 2-methylpyrrolidine-1-carboximidamide hydrochloride (**33**) (195 mg, 1.19 mmol). Water was added to the reaction, and the mixture was washed with DCM. The organic phase was then separated, dried, and concentrated in vacuo to give a residue, which was purified using flash column chromatography (0−5% MeOH/NH_3 in DCM) to give **36** as a light brown solid (167 mg, 72%): ^{1}H NMR ($CDCl_3$, 500 MHz) δ: 11.0 (s(b), 1H, OH), 5.60 (s, 1H, Ar H), 4.40−4.34 (m, 1H, CH), 3.72−3.67 (m, 1H, CH from CH_2), 3.50−3.45 (m, 1H, CH from CH_2), 2.17 (s, 3H, CH_3), 2.14−1.97 (m, 2H, 2× CH from CH_2), 1.75−1.70 (m, 1H, CH from CH_2), 1.24 (d, J = 6.3 Hz, 3H, CH_3); ^{13}C NMR ($CDCl_3$, 125 MHz) δ: 167.8 (C), 165.9 (C), 151.9 (C), 99.3 (CH), 53.6 (CH), 46.8 (CH_2), 32.6 (CH_2), 24.6 (CH_3), 23.2 (CH_2), 19.4 (CH_3); MS (ESI) m/z 194 $[M + H]^+$; HRMS (ESI) m/z: calcd for $C_{10}H_{15}N_3O^+$ $[M + H]^+$, 194.1288; found, 194.1309.

*6-Methyl-2-morpholinopyrimidin-4-ol (**37**).* General procedure G, from morpholine-4-carboximidamide hydrochloride (**34**) (97 mg, 0.59 mmol). Water was added to the reaction, and the mixture was washed with DCM. The organic phase was then separated, dried, and concentrated in vacuo to give a residue, which was purified using flash column chromatography (0−5% MeOH/NH_3 in DCM) to give **37** as an off-white solid (59 mg, 52%): ^{1}H NMR ($CDCl_3$, 500 MHz) δ: 12.0 (s(b), 1H, OH), 5.66 (s, 1H, Ar H), 3.81−3.79 (m, 4H, 2× CH_2), 3.76−3.74 (m, 4H, 2× CH_2), 2.18 (s, 3H, CH_3); ^{13}C NMR ($CDCl_3$, 125 MHz) δ: 167.7 (C), 166.2 (C), 153.8 (C), 100.8 (CH), 53.6 (CH), 66.5 (2× CH_2), 44.8 (2× CH_2), 24.4 (CH_3); MS (ESI) m/z 196 $[M + H]^+$; HRMS (ESI) m/z: calcd for $C_9H_{14}N_3O_2^+$ $[M + H]^+$, 196.1081; found, 196.1094.

*General Procedure H for the Formation of 5-Substituted Pyrimidine Analogues (Compounds **38, 39, and 42**).* To a solution of 3,5-dimethyl-1*H*-pyrazole-1-carboximidamide nitrate (1 equiv) in ethanol (0.65 M) were added the appropriate 1,3-dicarbonyls or acrylates (1.1 equiv) and NaOH (1.1 equiv). The reaction mixture was stirred overnight at 100 °C. Work-up and purification described individually in each example gave the intended product.

*2-(3,5-Dimethyl-1H-pyrazol-1-yl)-5-methylpyrimidin-4-ol (**38**).* General procedure H, using ethyl 2-methyl-3-oxopropanoate (**27**) (260 mg, 2.00 mmol). The reaction mixture was then cooled down to rt and concentrated in vacuo to give a residue, which was then purified with mass-directed HPLC to give **38** as a white solid (77 mg, 19%): ^{1}H NMR ($CDCl_3$, 500 MHz) δ: 10.6 (s(b), 1H, OH), 7.70 (s, 1H, Ar H), 6.04 (s, 1H, Ar H), 2.66 (s, 3H, CH_3), 2.26 (s, 3H, CH_3), 2.09 (s, 3H, CH_3); ^{13}C NMR ($CDCl_3$, 125 MHz) δ: 162.0 (C), 151.6 (C), 150.5 (CH), 146.8 (C), 143.3 (C), 121.0 (C), 111.2 (CH), 14.9 (CH_3), 13.6 (CH_3), 12.8 (CH_3); MS (ESI) m/z 216 $[M + H]^+$; HRMS (ESI) m/z: calcd for $C_{10}H_{13}N_4O^+$ $[M + H]^+$, 205.1084; found, 205.1111.

*Ethyl 2-(3,5-Dimethyl-1H-pyrazol-1-yl)-4-hydroxypyrimidine-5-carboxylate (**39**).* General procedure H, using diethyl 2-(ethoxymethylene)malonate (2.00 mL, 2.14 g, 9.89 mmol). The reaction mixture was then cooled down to rt, and the precipitate was filtered and washed with a minimal volume of cold ethanol to give **39** as a white solid (1.17 g, 50%): ^{1}H NMR (D_2O, 500 MHz) δ: 8.64 (s, 1H, Ar H), 6.09 (s, 1H, Ar H), 4.28 (q, J = 7.1 Hz, 2H, CH_2), 2.45 (s, 3H, CH_3), 2.18 (s, 3H, CH_3), 1.30 (t, J = 7.2 Hz, 3H, CH_3); ^{13}C NMR (D_2O, 125 MHz) δ: 172.5 (C), 168.1 (C), 160.1 (C), 158.2 (CH), 151.7 (C), 143.4 (C), 110.4 (C), 109.1 (CH), 61.6 (CH_2), 13.5 (CH_3), 12.8 (CH_3), 12.4 (CH_3); MS (ESI) m/z 263 $[M + H]^+$; HRMS (ESI) m/z: calcd for $C_{12}H_{15}N_4O_3^+$ $[M + H]^+$, 263.1139; found, 263.1161.

*2-(3,5-Dimethyl-1H-pyrazol-1-yl)-4-hydroxypyrimidine-5-carbonitrile (**42**).* General procedure H, using ethyl 2-cyano-3-ethoxyacrylate (433 mg, 2.56 mmol). The reaction mixture was then cooled down to rt, and the precipitate was filtered and washed with a minimal volume of cold ethanol. The precipitate was then redissolved in methanol and the solution was passed through an ion exchange column to remove any side products and give **42** as an off-white solid (142 mg, 28%): ^{1}H NMR ($CDCl_3$, 500 MHz) δ: 10.9 (s(b), 1H, OH), 8.31 (s, 1H, Ar H), 6.15 (s, 1H, Ar H), 2.68 (s, 3H, CH_3), 2.30 (s, 3H, CH_3); ^{13}C NMR ($CDCl_3$, 125 MHz) δ: 162.1 (CH), 157.5 (C), 154.7 (C), 150.5 (C), 145.0 (C), 113.6 (C), 113.4 (CH), 15.2 (CH_3), 13.7 (CH_3); MS (ESI) m/z 216 $[M + H]^+$; HRMS (ESI) m/z: calcd for $C_{10}H_{10}N_5O^+$ $[M + H]^+$, 216.0880; found, 216.0900.

Alternative Procedure Using Burgess Reagent. To a solution of 2-(3,5-dimethyl-1*H*-pyrazol-1-yl)-4-hydroxypyrimidine-5-carboxamide (**41**) (112 mg, 0.48 mmol) in THF (1 mL) was added Burgess reagent (286 mg, 1.20 mmol). The reaction mixture was stirred overnight at rt. The reaction mixture was concentrated in vacuo, and the residue was purified using mass-directed HPLC to give **42** as a white solid (21 mg, 20%).

*Methyl 2-(3,5-Dimethyl-1H-pyrazol-1-yl)-4-hydroxypyrimidine-5-carboxylate (**40**).* To a solution of ethyl 2-(3,5-dimethyl-1*H*-pyrazol-1-yl)-4-hydroxypyrimidine-5-carboxylate (**39**) (130 mg, 0.50 mmol) in methanol (2.5 mL) was added 7 M NH_3 in methanol (354 μL). The reaction mixture was stirred overnight at 75 °C. The reaction mixture was then concentrated in vacuo to give **40** as a white solid (125 mg, 102%): ^{1}H NMR (D_2O, 500 MHz) δ: 8.64 (s, 1H, Ar H), 6.09 (s, 1H, Ar H), 3.80 (s. 3H, CH_3), 2.42 (s, 3H, CH_3), 2.18 (s, 3H, CH_3); ^{13}C NMR (D_2O, 125 MHz) δ: 172.7 (C), 168.6 (C), 161.0 (CH), 158.4 (CH), 151.7 (C), 143.4 (C), 110.1 (C), 109.1 (CH), 52.0 (CH_3), 12.8 (CH_3), 12.4 (CH_3); MS (ESI) m/z 249 $[M + H]^+$; HRMS (ESI) m/z: calcd for $C_{11}H_{13}N_4O_3^+$ $[M + H]^+$, 249.0982; found, 249.0998.

*2-(3,5-Dimethyl-1H-pyrazol-1-yl)-4-hydroxypyrimidine-5-carboxamide (**41**).* Ethyl 2-(3,5-dimethyl-1*H*-pyrazol-1-yl)-4-hydroxypyrimidine-5-carboxylate (**39**) (183 mg, 0.70 mmol) was suspended in NH_4OH (3 mL). The suspension was then stirred at 75 °C overnight, of which the suspension became clear. The reaction mixture was then cooled to rt and was concentrated in vacuo to give **41** as a white solid (140 mg, 86%): ^{1}H NMR (MeOD, 500 MHz) δ: 8.77 (s, 1H, Ar H), 6.04 (s, 1H, Ar H), 2.60 (s, 3H, CH_3), 2.24 (s, 3H, CH_3); ^{13}C NMR (D_2O, 125 MHz) δ: 174.4 (C), 170.7 (C), 159.8 (CH), 159.5 (C), 151.5 (C), 144.2 (C), 111.9 (C), 110.2 (CH), 14.7 (CH_3), 13.5 (CH_3); MS (ESI) m/z 234 $[M + H]^+$; HRMS (ESI) m/z: calcd for $C_{10}H_{12}N_5O_2^+$ $[M + H]^+$, 234.0986; found, 234.0996.

*General Procedure I for the Coupling of Chloropyridines and 3,5-Dimethylpyrazoles (Compounds **43** and **44**).* To a solution of appropriate chloropyridine (1 equiv) in acetonitrile (0.6 M) were added 3,5-dimethylpyrazole (1 equiv), KOH (1

DOI: 10.1021/acsomega.9b02507
ACS Omega 2019, 4, 19199−19215

equiv), and 18-crown-6 (0.1 equiv). The reaction mixture was subjected to microwave irradiation at 80 °C. The reaction mixture was quenched with 2 M HCl, and the aqueous layer was extracted with ethyl acetate. The organic layer was then separated and concentrated in vacuo to give the residue, which was then purified using flash column chromatography (0−10% EtOAc in heptane) to give the intended product.

*2-Chloro-6-(3,5-dimethyl-1H-pyrazol-1-yl)-4-methylpyridine (**43**).* General procedure I, from 2,6-dichloro-4-methylpyridine (486 mg, 3.0 mmol), and subjected to microwave irradiation for 1.25 h. Chromatographic purification gave compound **43** as a white solid (331 mg, 50%): mp 45−46 °C; ^{1}H NMR ($CDCl_3$, 500 MHz) δ: 7.65 (s, 1H, Ar H), 7.01 (s, 1H, Ar H), 6.00 (s, 1H, Ar H), 2.67 (s, 3H, CH_3), 2.41 (s, 3H, CH_3), 2.31 (s, 3H, CH_3); ^{13}C NMR ($CDCl_3$, 125 MHz) δ: 152.9 (C), 152.5 (C), 150.3 (C), 148.7 (C), 142.2 (C), 121.3 (CH), 114.0 (CH), 109.5 (CH), 21.0 (CH_3), 14.7 (CH_3), 13.6 (CH_3); MS (ESI) m/z 222 $[M + H]^+$; HRMS (ESI) m/z: calcd for $C_{11}H_{13}N_3Cl^+$ $[M + H]^+$, 222.0793; found, 222.0803.

*2-Chloro-6-(3,5-dimethyl-1H-pyrazol-1-yl)pyridine (**44**).* General procedure I, from 2,6-dichloropyridine (444 mg, 3.0 mmol), and subjected to microwave irradiation for 2.25 h. Chromatographic purification gave compound **44** as a white solid (345 mg, 55%): mp 68−69 °C; ^{1}H NMR ($CDCl_3$, 500 MHz) δ: 7.83 (d, J = 8.1 Hz, 1H, Ar H), 7.73 (dd, J_1 = 7.9 Hz, J_2 = 7.9 Hz, 1H, Ar H), 7.16 (d, J = 7.7 Hz, 1H, Ar H), 6.01 (s, 1H, Ar H), 2.69 (s, 3H, CH_3), 2.31 (s, 3H, CH_3); ^{13}C NMR ($CDCl_3$, 125 MHz) δ: 153.1 (C), 150.5 (C), 148.7 (C), 142.2 (C), 140.5 (CH), 120.3 (CH), 113.2 (CH), 109.7 (CH), 14.8 (CH_3), 13.6 (CH_3); MS (ESI) m/z 208 $[M + H]^+$; HRMS (ESI) m/z: calcd for $C_{10}H_{11}N_3Cl^+$ $[M + H]^+$, 208.0636; found, 208.0642.

*General Procedure J for the Copper-Catalyzed Hydroxylation of Aryl Halides (Compounds **45** and **46**).* To a solution of the suitable aryl halide (1.0 equiv) in water (0.06 M) were added 55% tetrabutylammonium hydroxide (4.0 equiv), CuI (0.1 equiv), and 8-hydroxyquinoline 1-oxide (0.4 equiv). The reaction mixture was then subjected to microwave irradiation at 180 °C for 3 h. The reaction mixture was washed with ethyl acetate, and the organic phase was separated, dried, and concentrated in vacuo to give a residue, which was purified using flash column chromatography (0−25% EtOAc in heptane) to give the desired product.

*6-(3,5-Dimethyl-1H-pyrazol-1-yl)-4-methylpyridin-2-ol (**45**).* General procedure J, from 2-chloro-6-(3,5-dimethyl-1*H*-pyrazol-1-yl)-4-methylpyridine (**43**) (100 mg, 0.45 mmol) to give compound **45** as white solid (53 mg, 58%): mp 132−134 °C; ^{1}H NMR ($CDCl_3$, 500 MHz) δ: 9.52 (s(b), 1H, OH), 6.33 (s, 1H, Ar H), 6.31 (s, 1H, Ar H), 6.02 (s, 1H, Ar H), 2.50 (s, 3H, CH_3), 2.30 (s, 3H, CH_3), 2.27 (s, 3H, CH_3); ^{13}C NMR ($CDCl_3$, 125 MHz) δ: 162.2 (C), 153.1 (C), 150.5 (C), 142.9 (C), 140.4 (C), 113.1 (CH), 109.9 (CH), 100.1 (CH), 21.9 (CH_3), 13.8 (CH_3), 13.5 (CH_3); MS (ESI) m/z 204 $[M + H]^+$; HRMS (ESI) m/z: calcd for $C_{11}H_{14}N_3O^+$ $[M + H]^+$, 204.1131; found, 204.1148.

*6-(3,5-Dimethyl-1H-pyrazol-1-yl)pyridin-2-ol (**46**).* General procedure J, from 2-chloro-6-(3,5-dimethyl-1*H*-pyrazol-1-yl)-pyridine (**44**) (42 mg, 0.20 mmol) to give compound **46** as off-white solid (33 mg, 87%): mp 107−108 °C; ^{1}H NMR ($CDCl_3$, 500 MHz) δ: 9.83 (s(b), 1H, OH), 7.52 (dd, J_1 = 8.9 Hz, J_2 = 7.6 Hz, 1H, Ar H), 6.49 (d, J = 8.7 Hz, 1H, Ar H), 6.47 (d, J = 7.2 Hz, 1H, Ar H), 6.03 (s, 1H, Ar H), 2.50 (s, 3H, CH_3), 2.27 (s, 3H, CH_3); ^{13}C NMR ($CDCl_3$, 125 MHz) δ: 162.2 (C), 150.7 (C), 143.4 (C), 141.3 (CH), 140.5 (C), 113.9 (CH), 110.2 (CH), 97.5 (CH), 13.9 (CH_3), 13.5 (CH_3); MS (ESI) m/z 190 $[M + H]^+$; HRMS (ESI) m/z: calcd for $C_{10}H_{12}N_3O^+$ $[M + H]^+$, 190.0975; found, 190.0966.

Metabolomics. *General.* Compounds tested were obtained from commercial suppliers (marketed antibiotics) or in-house (hit compounds and analogues). *S. aureus* RN6390 was from in-house laboratory collection. LB were prepared in-house. All procedures were performed under aseptic conditions.

Determination of MIC via Microdilution Method. A series of dilution was prepared from a stock solution of compounds (dissolved in water/DMSO for known antibacterial drugs, DMSO for other synthetic in-house compounds) by diluting the stock solution with LB media. From each dilution, 100 μL was added into the wells of a 96-well plate. At the same time, the inoculum was prepared by making a 0.5 McFarland standard culture by diluting an overnight culture of *S. aureus* RN6390 with the appropriate media. The standard culture was then further diluted 100-fold with the same media. This diluted culture (100 μL) was added into the wells of a 96-well plate, bringing the final volume to 200 μL. The plate was covered with the lid provided and was incubated at 35−37 °C in air for 18−20 h. The MIC of the compound (averaged from two independent replicates) was defined as the lowest concentration of the compound, at which there was no visible growth.

Metabolomics Study of S. aureus RN6390 upon Exposure to Various Compounds with Antibacterial Activity. The metabolite extraction was adapted from Vincent et al.[17] Briefly, a 0.5 mL overnight culture of *S. aureus* RN6390 was inoculated into 49.5 mL of LB and the culture was incubated with shaking at 200 rpm at 37 °C. At 2 h, antibacterial compounds were added at 4× MIC. Samples were taken at 0, 1.5, and 3 h after the addition in 10 mL aliquots. Samples were cooled to 4 °C in a dry-ice-ethanol bath to quench metabolism before they were temporarily stored in ice. Cells (10 mL) were pelleted at 3894 relative centrifugal force (RCF), washed in 10 mL of cold 0.85% saline, and then resuspended in 1 mL of 0.85% saline. The OD_{600nm} of the cell suspension was taken and adjusted to 1. A 1 mL aliquot of cells was pelleted and resuspended in 200 μL of chloroform−methanol−water mixture (1:3:1, by volume) in a microcentrifuge tube. Acid-washed glass beads (200 μL) with the particle size ≤106 μm (Sigma-Aldrich) were added to the suspension, and the tube was shaken at 2000 rpm at 4 °C for 45 min (Eppendorf ThermoMixer C). The tube was subjected to a final centrifugation at 15871 RCF of which the supernatant was then taken and kept at −80 °C prior to data acquisition. Nine independent samples were generated for the untreated control, and three independent samples were generated for each treatment group. The data acquisition was similar to Vincent et al.[17] A 10 μL aliquot of each sample was run in a randomized order on a ZIC-pHILIC (polymeric hydrophilic interaction chromatography) column (Merck SeQuant) coupled to an Orbitrap mass spectrometer (Thermo Scientific) according to previously published methods.[51] Data analysis was performed using the MzMatch[52] and IDEOM[53] software packages for untargeted, initial analyses. PiMP[54] was used for further pathway analysis, generating $\log_2$ fold changes and peak verification. The PCA plot was generated using the MetaboAnalyst software.[47] Metabolomics data have been deposited to the EMBL-EBI MetaboLights database (DOI: 10.1093/nar/gks1004. PubMed PMID: 23109552) with the identifier MTBLS788.

DOI: 10.1021/acsomega.9b02507
ACS Omega 2019, 4, 19199−19215

■ ASSOCIATED CONTENT

Supporting Information

The Supporting Information is available free of charge on the ACS Publications website at DOI: 10.1021/acsomega.9b02507.

Notes on analysis of the data from the whole cell screening, NMR data to show the structure of key compounds, physicochemical data of key compounds, activity data of selected compounds against different strains of *S. aureus*, further metabolomic data on ciprofloxacin and trimethoprim (PDF)

■ AUTHOR INFORMATION

Corresponding Author

*E-mail: i.h.gilbert@dundee.ac.uk. Tel: +44 1382 386 240.

ORCID

Ian H. Gilbert: 0000-0002-5238-1314

Notes

The authors declare no competing financial interest.

■ ACKNOWLEDGMENTS

This research is part-funded by the MSD Scottish Life Sciences fund (A.S.T.L.). As a part of an on-going contribution to Scottish life sciences, Merck Sharp & Dohme Limited (MSD, tradename of Merck & Co., Inc., Kenilworth, New Jersey) a global healthcare leader, has given substantial monetary funding to the Scottish Funding Council (SFC) for distribution via the Scottish Universities Life Science Alliance (SULSA) to develop and deliver a high-quality drug discovery research and training program. All aspects of the program have been geared toward attaining the highest value in terms of scientific discovery, training, and impact. The opinions expressed in this research are those of the authors and neither represent those of MSD nor its Affiliates. The authors would also like to acknowledge the help of Erin Manson from Glasgow Polyomics, University of Glasgow for technical assistance.

■ REFERENCES

(1) Okeke, I. N.; Laxminarayan, R.; Bhutta, Z. A.; Duse, A. G.; Jenkins, P.; O'Brien, T. F.; Pablos-Mendez, A.; Klugman, K. P. Antimicrobial resistance in developing countries. Part I: recent trends and current status. *Lancet Infect. Dis.* **2005**, *5*, 481−493.

(2) Laxminarayan, R.; Duse, A.; Wattal, C.; Zaidi, A. K.; Wertheim, H. F.; Sumpradit, N.; Vlieghe, E.; Hara, G. L.; Gould, I. M.; Goossens, H.; Greko, C.; So, A. D.; Bigdeli, M.; Tomson, G.; Woodhouse, W.; Ombaka, E.; Peralta, A. Q.; Qamar, F. N.; Mir, F.; Kariuki, S.; Bhutta, Z. A.; Coates, A.; Bergstrom, R.; Wright, G. D.; Brown, E. D.; Cars, O. Antibiotic resistance-the need for global solutions. *Lancet Infect. Dis.* **2013**, *13*, 1057−1098.

(3) O'Neill, J. *The Review on Antimicrobial Resistance*; 2016, https://amr-review.org.

(4) The Pew Charitable Trusts. *Antibiotics Currently in Clinical Development*, 2016. http://www.pewtrusts.org/~/media/assets/2016/12/antibiotics_datatable_201612.pdf.

(5) Hay, M.; Thomas, D. W.; Craighead, J. L.; Economides, C.; Rosenthal, J. Clinical development success rates for investigational drugs. *Nat. Biotechnol.* **2014**, *32*, 40−51.

(6) Walsh, C. T.; Fischbach, M. A. Antibiotics for emerging pathogens. *Science* **2009**, *325*, 1089−1093.

(7) Silver, L. L. Challenges of Antibacterial Discovery. *Clin. Microbiol. Rev.* **2011**, *24*, 71−108.

(8) Silver, L. L. A Gestalt approach to Gram-negative entry. *Bioorg. Med. Chem.* **2016**, *24*, 6379−6389.

(9) Mugumbate, G.; Overington, J. P. The relationship between target-class and the physicochemical properties of antibacterial drugs. *Bioorg. Med. Chem.* **2015**, *23*, 5218−5224.

(10) O'Shea, R.; Moser, H. E. Physicochemical properties of antibacterial compounds: implications for drug discovery. *J. Med. Chem.* **2008**, *51*, 2871−2878.

(11) Ebejer, J. P.; Charlton, M. H.; Finn, P. W. Are the physicochemical properties of antibacterial compounds really different from other drugs? *J. Cheminf.* **2016**, *8*, No. 30.

(12) Brown, D. G.; May-Dracka, T. L.; Gagnon, M. M.; Tommasi, R. Trends and exceptions of physical properties on antibacterial activity for Gram-positive and Gram-negative pathogens. *J. Med. Chem.* **2014**, *57*, 10144−10161.

(13) Hann, M. M.; Leach, A. R.; Harper, G. Molecular complexity and its impact on the probability of finding leads for drug discovery. *J. Chem. Inf. Comput. Sci.* **2001**, *41*, 856−864.

(14) Leach, A. R.; Hann, M. M. Molecular complexity and fragment-based drug discovery: ten years on. *Curr. Opin. Chem. Biol.* **2011**, *15*, 489−496.

(15) Nadin, A.; Hattotuwagama, C.; Churcher, I. Lead-Oriented Synthesis: A New Opportunity for Synthetic Chemistry. *Angew. Chem., Int. Ed.* **2012**, *51*, 1114−1122.

(16) Fiehn, O. Metabolomics–the link between genotypes and phenotypes. *Plant Mol. Biol.* **2002**, *48*, 155−171.

(17) Vincent, I. M.; Ehmann, D. E.; Mills, S. D.; Perros, M.; Barrett, M. P. Untargeted Metabolomics To Ascertain Antibiotic Modes of Action. *Antimicrob. Agents Chemother.* **2016**, *60*, 2281−2291.

(18) Zampieri, M.; Szappanos, B.; Buchieri, M. V.; Trauner, A.; Piazza, I.; Picotti, P.; Gagneux, S.; Borrell, S.; Gicquel, B.; Lelievre, J.; Papp, B.; Sauer, U. High-throughput metabolomic analysis predicts mode of action of uncharacterized antimicrobial compounds. *Sci. Transl. Med.* **2018**, *10*, No. eaal3973.

(19) Campos, A. I.; Zampieri, M. Metabolomics-Driven Exploration of the Chemical Drug Space to Predict Combination Antimicrobial Therapies. *Mol. Cell* **2019**, *74*, 1291.e6−1303.e6.

(20) Belenky, P.; Ye, J. D.; Porter, C. B.; Cohen, N. R.; Lobritz, M. A.; Ferrante, T.; Jain, S.; Korry, B. J.; Schwarz, E. G.; Walker, G. C.; Collins, J. J. Bactericidal Antibiotics Induce Toxic Metabolic Perturbations that Lead to Cellular Damage. *Cell Rep.* **2015**, *13*, 968−980.

(21) Zampieri, M.; Zimmermann, M.; Claassen, M.; Sauer, U. Nontargeted Metabolomics Reveals the Multilevel Response to Antibiotic Perturbations. *Cell Rep.* **2017**, *19*, 1214−1228.

(22) Ray, P. C.; Kiczun, M.; Huggett, M.; Lim, A.; Prati, F.; Gilbert, I. H.; Wyatt, P. G. Fragment library design, synthesis and expansion: nurturing a synthesis and training platform. *Drug Discovery Today* **2017**, *22*, 43−56.

(23) Napper, A. D.; Hixon, J.; McDonagh, T.; Keavey, K.; Pons, J. F.; Barker, J.; Yau, W. T.; Amouzegh, P.; Flegg, A.; Hamelin, E.; Thomas, R. J.; Kates, M.; Jones, S.; Navia, M. A.; Saunders, J.; DiStefano, P. S.; Curtis, R. Discovery of indoles as potent and selective inhibitors of the deacetylase SIRT1. *J. Med. Chem.* **2005**, *48*, 8045−8054.

(24) Gertz, M.; Fischer, F.; Nguyen, G. T. T.; Lakshminarasimhan, M.; Schutkowski, M.; Weyand, M.; Steegborn, C. Ex-527 inhibits Sirtuins by exploiting their unique NAD(+)-dependent deacetylation mechanism. *Proc. Natl. Acad. Sci. U.S.A.* **2013**, *110*, E2772−E2781.

(25) Chen, D.; Errey, J. C.; Heitman, L. H.; Marshall, F. H.; IJzerman, A. P.; Siegal, G. Fragment Screening of GPCRs Using Biophysical Methods: Identification of Ligands of the Adenosine A(2A) Receptor with Novel Biological Activity. *ACS Chem. Biol.* **2012**, *7*, 2064−2073.

(26) Chen, D.; Ranganathan, A.; Ijzerman, A. P.; Siegal, G.; Carlsson, J. Complementarity between in Silico and Biophysical Screening Approaches in Fragment-Based Lead Discovery against the A(2A) Adenosine Receptor. *J. Chem. Inf. Model.* **2013**, *53*, 2701−2714.

DOI: 10.1021/acsomega.9b02507
ACS Omega 2019, 4, 19199−19215

(27) Montalbetti, N.; Simonin, A.; Simonin, C.; Awale, M.; Reymond, J. L.; Hediger, M. A. Discovery and characterization of a novel non-competitive inhibitor of the divalent metal transporter DMT1/SLC11A2. *Biochem. Pharmacol.* **2015**, *96*, 216−224.
(28) Nishimura, T.; Miyamoto, Y.; Ohyama, H.; Yamamura, H.; Morita, K.; Matsumoto, K.; Watanabe, T. Pyrazolylpyrimidine Derivatives. US4405743A, 1983.
(29) Konishi, K.; Kuragano, T. Studies on Fungicidal Pyrimidinylhydrazones .5. Fungicidal Activity of Pyrazolylpyrimidines. *J. Pestic. Sci.* **1990**, *15*, 13−22.
(30) https://pubchem.ncbi.nlm.nih.gov/bioassay/1626.
(31) Galvão, T. L. P.; Rocha, I. M.; Ribeiro da Silva, M. D M. C.; Ribeiro da Silva, M. A. V. From 2-hydroxypyridine to 4(3H)-pyrimidinone: computational study on the control of the tautomeric equilibrium. *J. Phys. Chem. A* **2013**, *117*, 12668−12674.
(32) Slanina, Z.; Leś, A.; Adamowicz, L. Complexes of 4-aminopyrimidine and 4-hydroxypyrimidine with water: computed relative thermodynamic stabilities. *Thermochim. Acta* **1994**, *231*, 61−68.
(33) Erkin, A. V.; Krutikov, V. I. Formation, structure and heterocyclization of aminoguanidine and ethyl acetoacetate condensation products. *Russ. J. Gen. Chem.* **2009**, *79*, 1204−1209.
(34) Nishigaki, S.; Senga, K.; Aida, K.; Takabata, T.; Yoneda, F. Condensation Reactions of Ethyl Ethyoxymethylenecyanoacetate with Amidines. *Chem. Pharm. Bull.* **1970**, *18*, 1003.
(35) Lorente, A.; Vaquerizo, L.; Martin, A.; Gomezsal, P. Regioselective Synthesis of Pyrimidines from Ketene Dithioacetals or Alkoxymethylene Compounds. *Heterocycles* **1995**, *41*, 71−86.
(36) Yang, K.; Li, Z.; Wang, Z. Y.; Yao, Z. Y.; Jiang, S. Highly Efficient Synthesis of Phenols by Copper-Catalyzed Hydroxylation of Aryl Iodides, Bromides, and Chlorides. *Org. Lett.* **2011**, *13*, 4340−4343.
(37) Wang, Y. X.; Zhou, C. S.; Wang, R. H. Copper-catalyzed hydroxylation of aryl halides: efficient synthesis of phenols, alkyl aryl ethers and benzofuran derivatives in neat water. *Green Chem.* **2015**, *17*, 3910−3915.
(38) Hopkins, A. L.; Keseru, G. M.; Leeson, P. D.; Rees, D. C.; Reynolds, C. H. The role of ligand efficiency metrics in drug discovery. *Nat. Rev. Drug Discovery* **2014**, *13*, 105−121.
(39) Booth, M. C.; Cheung, A. L.; Hatter, K. L.; Jett, B. D.; Callegan, M. C.; Gilmore, M. S. Staphylococcal accessory regulator (sar) in conjunction with agr contributes to *Staphylococcus aureus* virulence in endophthalmitis. *Infect. Immun.* **1997**, *65*, 1550−1556.
(40) Cheung, A. L.; Eberhardt, K. J.; Chung, E.; Yeaman, M. R.; Sullam, P. M.; Ramos, M.; Bayer, A. S. Diminished Virulence of a Sar(-)/Agr(-) Mutant of *Staphylococcus aureus* in the Rabbit Model of Endocarditis. *J. Clin. Invest.* **1994**, *94*, 1815−1822.
(41) Kahl, B. C.; Goulian, M.; Van Wamel, W.; Herrmann, M.; Simon, S. M.; Kaplan, G.; Peters, G.; Cheung, A. L. *Staphylococcus aureus* RN6390 replicates and induces apoptosis in a pulmonary epithelial cell line. *Infect. Immun.* **2000**, *68*, 5385−5392.
(42) Nair, D.; Memmi, G.; Hernandez, D.; Bard, J.; Beaume, M.; Gill, S.; Francois, P.; Cheung, A. L. Whole-genome sequencing of *Staphylococcus aureus* strain RN4220, a key laboratory strain used in virulence research, identifies mutations that affect not only virulence factors but also the fitness of the strain. *J. Bacteriol.* **2011**, *193*, 2332−2335.
(43) Stipetic, L. H.; Dalby, M. J.; Davies, R. L.; Morton, F. R.; Ramage, G.; Burgess, K. E. V. A novel metabolomic approach used for the comparison of *Staphylococcus aureus* planktonic cells and biofilm samples. *Metabolomics* **2016**, *12*, No. 75.
(44) Meyer, H.; Liebeke, M.; Lalk, M. A protocol for the investigation of the intracellular *Staphylococcus aureus* metabolome. *Anal. Biochem.* **2010**, *401*, 250−259.
(45) Liebeke, M.; Meyer, H.; Donat, S.; Ohlsen, K.; Lalk, M. A metabolomic view of *Staphylococcus aureus* and its Ser/Thr kinase and phosphatase deletion mutants: involvement in cell wall biosynthesis. *Chem. Biol.* **2010**, *17*, 820−830.
(46) Dörries, K.; Schlueter, R.; Lalk, M. Impact of Antibiotics with Various Target Sites on the Metabolome of Staphylococcus aureus. *Antimicrob. Agents Chemother.* **2014**, *58*, 7151−7163.
(47) Xia, J.; Wishart, D. S. Using MetaboAnalyst 3.0 for Comprehensive Metabolomics Data Analysis. *Curr. Protoc. Bioinf.* **2016**, *55*, 14.10.11−14.10.91.
(48) Nonejuie, P.; Burkart, M.; Pogliano, K.; Pogliano, J. Bacterial cytological profiling rapidly identifies the cellular pathways targeted by antibacterial molecules. *Proc. Natl. Acad. Sci. U.S.A.* **2013**, *110*, 16169−16174.
(49) Kenzo, S. Google Patents, 1962.
(50) El-Mansy, M. F.; Kang, J. Y.; Lingampally, R.; Carter, R. G. Proline Sulfonamide-Catalyzed, Domino Process for Asymmetric Synthesis of Amino- and Hydroxy-Substituted Bicyclo[2.2.2]octanes. *Eur. J. Org. Chem.* **2016**, 150−157.
(51) Vincent, I. M.; Creek, D. J.; Burgess, K.; Woods, D. J.; Burchmore, R. J. S.; Barrett, M. P. Untargeted Metabolomics Reveals a Lack Of Synergy between Nifurtimox and Eflornithine against Trypanosoma brucei. *PLoS Neglected Trop. Dis.* **2012**, *6*, No. e1618.
(52) Scheltema, R. A.; Jankevics, A.; Jansen, R. C.; Swertz, M. A.; Breitling, R. PeakML/mzMatch: A File Format, Java Library, R Library, and Tool-Chain for Mass Spectrometry Data Analysis. *Anal. Chem.* **2011**, *83*, 2786−2793.
(53) Creek, D. J.; Jankevics, A.; Burgess, K. E. V.; Breitling, R.; Barrett, M. P. IDEOM: an Excel interface for analysis of LC-MS-based metabolomics data. *Bioinformatics* **2012**, *28*, 1048−1049.
(54) Gloaguen, Y.; Morton, F.; Daly, R.; Gurden, R.; Rogers, S.; Wandy, J.; Wilson, D.; Barrett, M.; Burgess, K. PiMP my metabolome: an integrated, web-based tool for LC-MS metabolomics data. *Bioinformatics* **2017**, *33*, 4007−4009.

DOI: 10.1021/acsomega.9b02507
ACS Omega 2019, 4, 19199−19215